



ELSEVIER

Palaeogeography, Palaeoclimatology, Palaeoecology 169 (2001) 129–152

PALAEO

www.elsevier.nl/locate/palaeo

Molecular fossil constraints on the water column structure of the Cenomanian–Turonian Western Interior Seaway, USA

Dirk-Jan H. Simons, Fabien Kenig*

University of Illinois at Chicago, Department of Earth and Environmental Sciences, M/C 186, 845 West Taylor Street, Chicago, IL 60607-7059, USA

Received 24 May 2000; accepted for publication 24 January 2001

Abstract

Bulk-geochemical and biomarker (molecular fossil) data were collected for four Cenomanian–Turonian sections in the Western Interior Basin, USA. The four sections represent a 900 km wide transect across the basin from Kansas to New Mexico. Rock–Eval and biomarker analyses indicate an east–west thermal maturity trend due to progressive deeper burial associated with the tectonic flexure of the foreland basin since the Cenomanian–Turonian. At each site the source of extractable organic matter is dominantly marine with minor terrestrial contribution. The presence of isorenieratene derivatives in samples from Bunker Hill (KS), Pueblo (CO), and Red Wash (NM) indicates the presence of the green sulfur bacterium *Chlorobium* in the water column, and shows that the southern part of the Western Interior Seaway (WIS) experienced events of photic zone anoxia. At maximum transgression, sedimentary features indicative of water column oxygenation occur within single beds with geochemical evidence of photic zone anoxia. This is consistent with a scenario in which bottom waters experienced alternating oxic/dysoxic and anoxic conditions. These so-called ‘intermittent anoxic events’ underline the high variability in redox conditions in the WIS. The distribution of isorenieratene derivatives shows a dynamic water column structure of the WIS, and indicates that anoxia was a permanent feature of the transgressive and regressive intervals of the Greenhorn Cyclothem, rather than at maximum transgression. Hence, the oceanographic circulation is dominated by near field effects inherent to the seaway, rather than by direct proto-Atlantic elements such as the oceanic anoxic event (OAE). © 2001 Elsevier Science B.V. All rights reserved.

Keywords: Biomarkers; Anoxic environment; Cenomanian; Turonian; Epeiric seas

1. Introduction

High global sea level during the Jurassic and Cretaceous resulted in the formation of extensive epeiric seas. The Western Interior Seaway (WIS) extended approximately 6000 km meridionally over the central North American continent throughout most of the Cretaceous (e.g. Kauffman and Caldwell,

1993; Fig. 1), providing a conduit between the sub-mediterranean Boreal Sea and subtropical water masses from the proto-Gulf of Mexico and Atlantic Ocean (Tethys). The WIS resulted from the development of an elongated foreland basin east of the emerging North American Cordillera in conjunction with the highest global sea levels of Mesozoic times (Monger, 1993; Kauffman and Caldwell, 1993).

Although the Cretaceous saw the waxing and waning of several trans-continental seaways in different climatic settings such as the trans-African- (Reyment, 1980); the trans-Asian-, and the trans-Australian

* Corresponding author. Tel.: +1-312-996-3020, fax: +1-312-413-2279.

E-mail address: fkenig@uic.edu (F. Kenig).

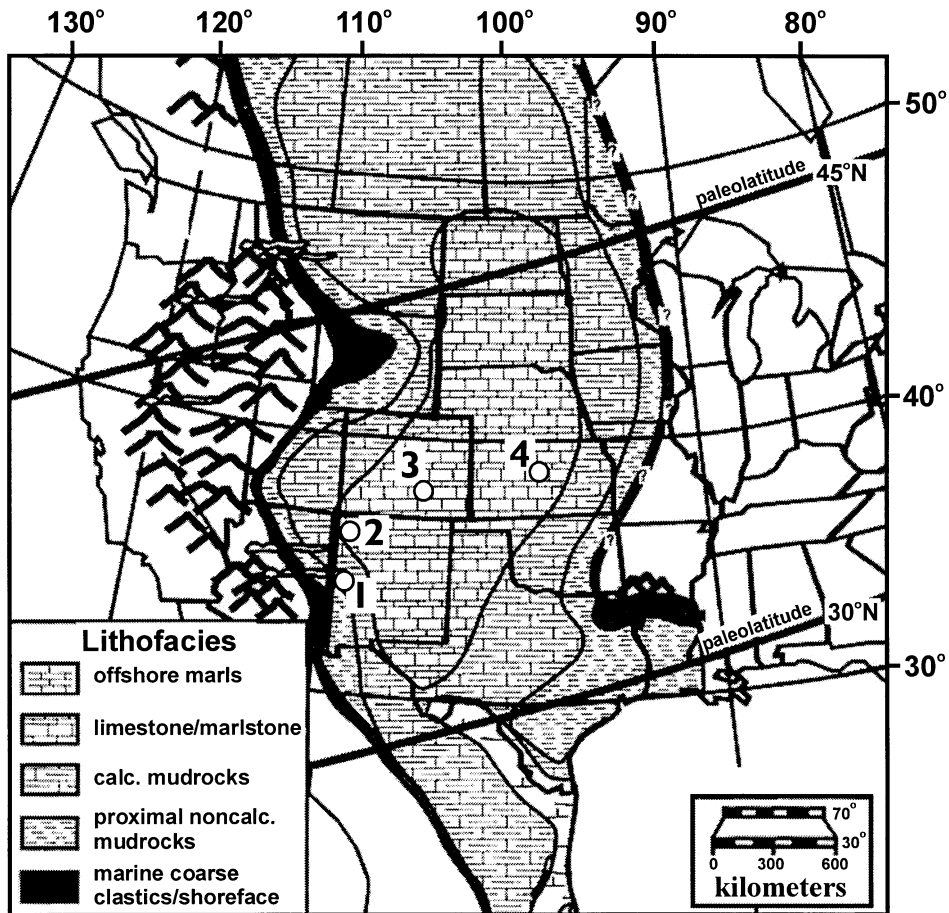


Fig. 1. Lithofacies map of the WIS at maximum transgression (early Turonian; adapted from Dean and Arthur, 1998). Numbers indicate sampling locations: (1) Mueses Canyon, New Mexico; (2) Red Wash, New Mexico; (3) Pueblo, Colorado; (4) Bunker Hill, Kansas.

epeiric seas (Veevers, 1984), all providing relatively shallow conduits between marine basins, the paleoceanography of these settings is relatively unique. Compared to its contemporaneous equivalents, the WIS was by far the most extensive especially during the Cenomanian–Turonian second order sea level cycle known as the Greenhorn Cyclothem (Kauffman, 1977). In contrast, Cenozoic and recent marginal marine and epicontinental settings either have a single connection to an open marine environment or are openly connected to an oceanic basin (Hay et al., 1993). There are no modern analogs to the WIS, although it has been suggested that oceanographic conditions of this seaway are somewhat similar to large estuarine systems (Slingerland et al., 1996).

Paleoceanographic circulation in the WIS has been constrained mostly by paleontologic data (e.g. Caldwell and Kauffman, 1993 and references therein; Leckie et al., 1998) and by atmospheric circulation models (Ericksen and Slingerland, 1990; Slingerland et al., 1996; Kump and Slingerland, 1999). The upper Cretaceous marine biota of the Western Interior Basin are represented by well-preserved, widespread, and well-studied macro- and micro-faunas (e.g. Kauffman, 1973, 1975, 1984; Pratt, 1985; Caldwell and Kauffman, 1993; Schröder-Adams et al., 1996), which indicate restricted marine conditions, uncharacteristic of open oceanic basins. Two factors are indicated to account for non-normal marine conditions. The first factor is water column stratification

throughout a considerable part of the basin's history (Kauffman and Sageman, 1990). This gave way to dysoxic to anoxic bottom-water environments supporting relatively abundant opportunistic and low-oxygen-adapted taxa (Sageman et al., 1991; Mieras et al., 1993; Savrda and Bottjer, 1993). The second factor inferred from biota is the predominance of brackish-water conditions for surface waters with influx of cooler, less-saline waters from the northern circumpolar ocean (Hay et al., 1993). This inferred freshwater influence, even in shallower fully oxygenated waters, is reflected in marine biofacies with low diversity and paucity of typical marine organisms, such as skeletonized sponges, bryozoans, brachiopods, corals, and echinoderms (Sohl, 1967; Kauffman, 1984). However, it is suggested that around the Cenomanian–Turonian peak sea-level highstand, warm subtropical to warm-temperate marine water masses from the proto-Gulf of Mexico rapidly spread northward into the basin (Eicher and Diner, 1985; Elder, 1985, 1991; Elder and Kirkland, 1985; Bralower, 1988; Kauffman and Caldwell, 1993). Consequently, a full complement of normal marine foraminiferal assemblages is associated with these water masses (Kauffman, 1984; Cobban, 1993).

In contrast, the distribution of planktic and benthic foraminifera during the Greenhorn Cyclothem led several authors to suggest an incursion of a Tethyan-derived oxygen minimum zone (OMZ) into the seaway around the Cenomanian–Turonian highstand, impeding the development open marine biota (Frush and Eicher, 1975; Elder, 1987; Leckie, 1985; Leckie et al., 1991, 1998). The Cenomanian–Turonian boundary coincides with an oceanic anoxic event (OAE) which is expressed globally as a positive excursion of the stable carbon isotopic composition of carbonates and organic carbon (Schlanger and Jenkyns, 1976; Pratt, 1985; Schlanger et al., 1987; Arthur et al., 1988; Hayes et al., 1989).

Paleoceanographic reconstruction of the WIS is also based on atmospheric circulation models, but was limited to the early Turonian (Slingerland et al., 1996; Kump and Slingerland, 1999). These models have insufficient temporal and spatial resolution to capture the variability of observed sedimentary features (e.g. laminated shale to calcareous shale–limestone bed couplets). For example, Kump and Slingerland (1999) concluded that the existing paleo-

ceanographic models for the WIS based on atmospheric circulation “cannot generate the stable water column condition necessary to generate bottom water anoxia”. Hence, there exists a noticeable discordance between paleoceanographic circulation inferences from paleontologic data and numerical atmosphere–ocean models, and additional constraints are necessary. This contribution provides new molecular fossil (biomarker) data from a cross-basinal transect of the southern WIS, which renders insight on the evolution of water column conditions. Four Cenomanian–Turonian sections from Kansas (Bunker Hill), Colorado (Pueblo), and New Mexico (Red Wash and Mueses Canyon) were studied with a combined approach of biomarker analyses and bulk-geochemical data, to deconvolute the thermal history, source, and depositional environment of organic matter from the Greenhorn Cyclothem of the WIS. Association of paleontological and sedimentological data to organic geochemical data helps to resolve the water column structure and its evolution and, thus, provides new boundary conditions for paleoceanographic circulation reconstruction. Specifically, we use the distribution of isorenieratene derivatives to determine unambiguously the presence of *Chlorobiaceae*, photosynthetic green sulfur bacteria, in the environment of deposition (Summons and Powell, 1986). The presence of *Chlorobiaceae*, organisms living in anoxic waters below the chemocline but within the photic zone, provides a strong constraint on water column stratification: anoxic bottom water mass reaching up into the photic zone (e.g. Sinninghe Damsté et al., 1993). Therefore, the distribution of isorenieratene derivatives in the studied sections helps to resolve the interplay between oxic/dysoxic and anoxic bottom waters for the WIS.

2. Samples

Four sections of the Greenhorn Cyclothem were sampled in the Western USA to obtain a representative cross-basinal transect of the southern WIS around the Cenomanian–Turonian boundary. Samples were collected from outcrops at Mueses Canyon and Red Wash (New Mexico), Pueblo (Colorado), and Bunker Hill (Kansas; Fig. 1). The samples from Bunker Hill were collected on the section described by Hattin

(1975) near the Wilson Reservoir (west line, sec. 18, T. 13S, R. 12W, Russell County), and on Canyon Road (north line, sec. 1, T. 13S, R. 15W, Russell County). The Pueblo samples were collected at the type section along the Arkansas River in Lake Pueblo State Park (Pratt, 1985). The Red Wash samples were collected in the Navajo Reservation at the Four Corners area near Farmington. The exact location of the Red Wash section is provided by Curiale (1994a,b). Mueses Canyon samples comprise silty shales of the middle Cenomanian Whitewater Arroyo Shale (Wolfe, 1989).

Figs. 2A, 3A and 4A show schematic stratigraphic sections at Bunker Hill, KS; Pueblo, CO; and Red Wash, NM, respectively. The sampled sections encompass depositional cycles within the second order eustatic Greenhorn Cyclothem of limestone and shale beds (Kauffman, 1977; Hancock and Kauffman, 1979) and include the Graneros Shale (in KS and CO), the Mancos Shale (in NM), and the Greenhorn Formation (in KS, CO, and NM). These sections have been described in detail previously (e.g. Molenaar, 1977; Hattin, 1965, 1975; Pratt et al., 1985). The transect spans approximately 900 km. Stratigraphic correlation across the basin is provided by bentonite marker beds (Elder, 1985 and Elder et al., 1994).

3. Methods

To obtain total organic carbon (TOC) content, Hydrogen index (HI, mg HC/g TOC), Oxygen Index (OI, mg CO₂/g TOC), T_{\max} (°C), and carbonate carbon content, Rock-Eval analyses was performed on 122 samples at Institut Français du Pétrole on Rock-Eval/6, following the method described by Espitalié et al. (1977) and Lafargue et al. (1997). Finely powdered sediment samples were Soxhlett extracted with dichloromethane/methanol (7.5:1, v/v) for 72 h. Total extracts were separated by column chromatography into fractions following the analytical flow diagram (Fig. 5) adapted from Kenig et al. (1995). Polar fractions were desulfurized using nickel boride following the method described by Schouten et al. (1993). The resulting saturated hydrocarbon, aromatic and desulfurized hydrocarbon fractions were analyzed by gas chromatography coupled to a flame ionization detec-

tor (GC-FID), and gas chromatography-mass spectrometry (GC-MS).

GC-FID was performed using a Hewlett-Packard 5890 series II Plus equipped with a split/splitless injector operated in splitless mode. A 30 m Hewlett-Packard HP-5MS fused silica capillary column (0.25 mm id, 0.25 μ m film thickness) was used with helium as carrier gas. Samples were injected at 60°C, held for 1.5 min, and the oven temperature was programmed to 130°C at 20°C/min, and then at 4°C/min to 315°C, at which it was held for 88 min.

GC-MS was performed on a Hewlett-Packard 6890 gas chromatograph coupled to a Hewlett-Packard 5973 mass selective detector (MSD) operated in electron-impact mode at 70 eV, scanning a mass range of m/z 40–650 at 2.44 scans per second. A HP-5MS capillary column (30 m \times 0.25 mm \times 0.25 μ m) was used, and the oven temperature program was identical to the GC-FID method described above. Helium was used as carrier gas, and injection was performed in pulsed-splitless mode.

For quantification purposes, 10 nmol of perdeuterated external standards (anthracene and *n*-eicosane) per mg of sample fraction were co-injected during GC-FID and GC-MS analyses. Isorenieratane **I** (roman numbers represent structures shown in Appendix A) was quantified by integration of the corresponding peak in the summed mass chromatograms m/z 133 + m/z 134, and compared with the peak area of the standard (perdeuterated anthracene) in the mass chromatogram m/z 188. The major fragment ions of isorenieratane are m/z 133 and 134 (Schaeffle et al., 1977; Hartgers et al., 1994), and thus, the peak area of isorenieratane in the summed mass chromatogram m/z 133 + m/z 134 is representative for the concentration of the whole molecule. Similarly, m/z 188 is the major fragment ion for perdeuterated anthracene, thus its concentration is determined by integrating the peak area for that compound in the mass chromatogram m/z 188. This method of quantification provides relative, rather than absolute, concentrations as incomplete fragmentation and ion-losses within the mass spectrometer are likely to occur and are not necessarily similar for different molecules. Hence, the isorenieratane concentration profiles in Figs. 3C and 4C do not have units.

Odd-over-even-predominance of *n*-alkanes were

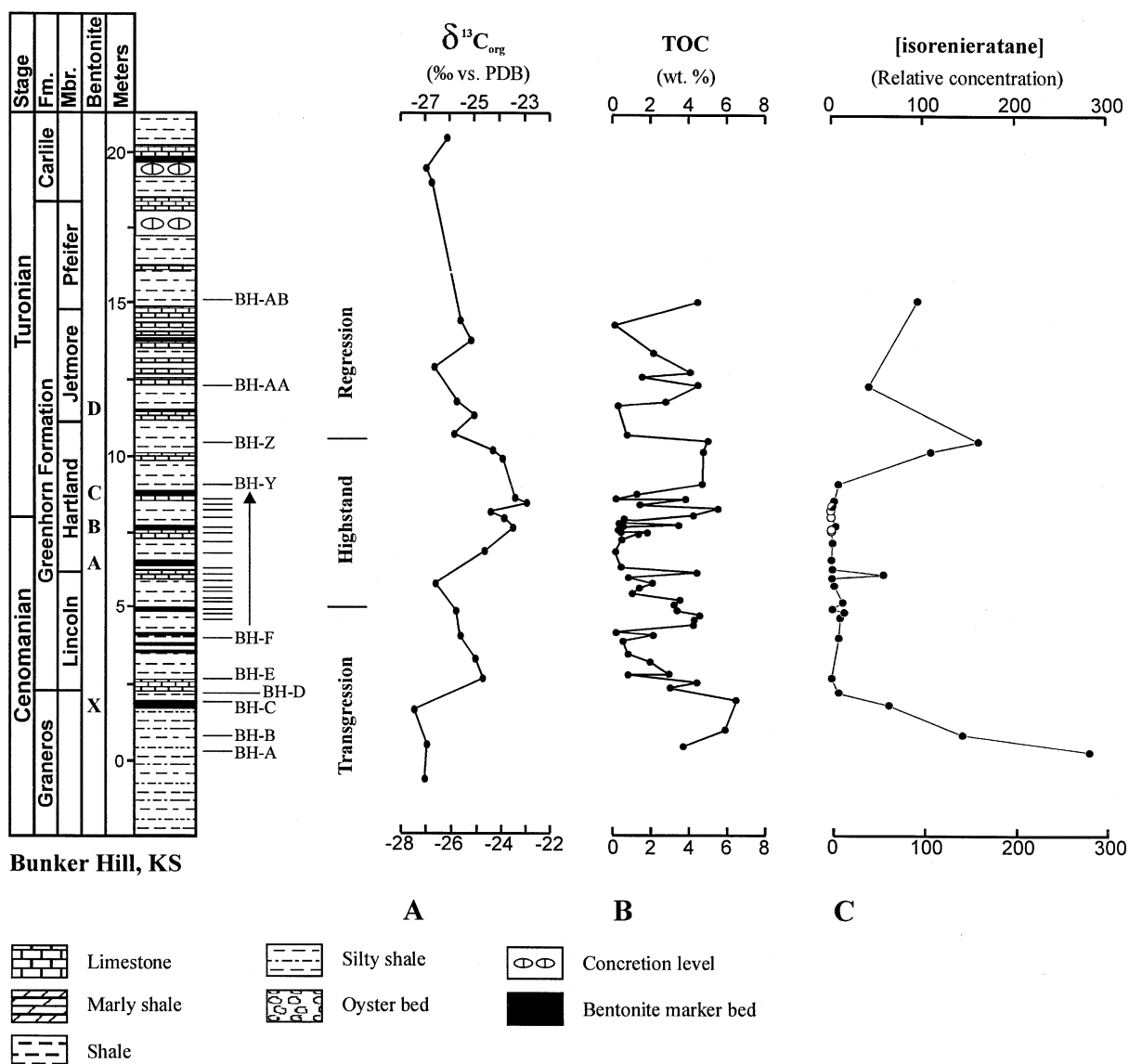


Fig. 2. Schematic stratigraphic column of the Cenomanian–Turonian outcrop at Bunker Hill, Kansas. (A) $\delta^{13}C_{org}$ profile (Pratt et al., 1985). (B) TOC content (TOC, in wt%) profile obtained from Rock–Eval analyses. (C) Relative concentration profile of isorenieratane: solid circles represent the presence of isorenieratane and aryl-isoprenoids, semi-solid circles represent the presence of aryl-isoprenoids only, and open circles indicate the absence of isorenieratane derivatives.

determined by calculating a running OEP value based on peak areas of integrated peaks in the m/z 57 mass chromatogram of saturated hydrocarbon fractions, using the following equation (Scalan and Smith, 1970): $OEP_x = (C_{(x-2)} + 6C_x + C_{(x+2)}) / (4C_{(x-1)} + 4C_{(x+1)})$, where x is the carbon number.

4. Results

4.1. Total organic carbon (TOC) content

TOC profiles of the Bunker Hill, Pueblo, and Red Wash sections are shown in Figs. 2B, 3B and 4B

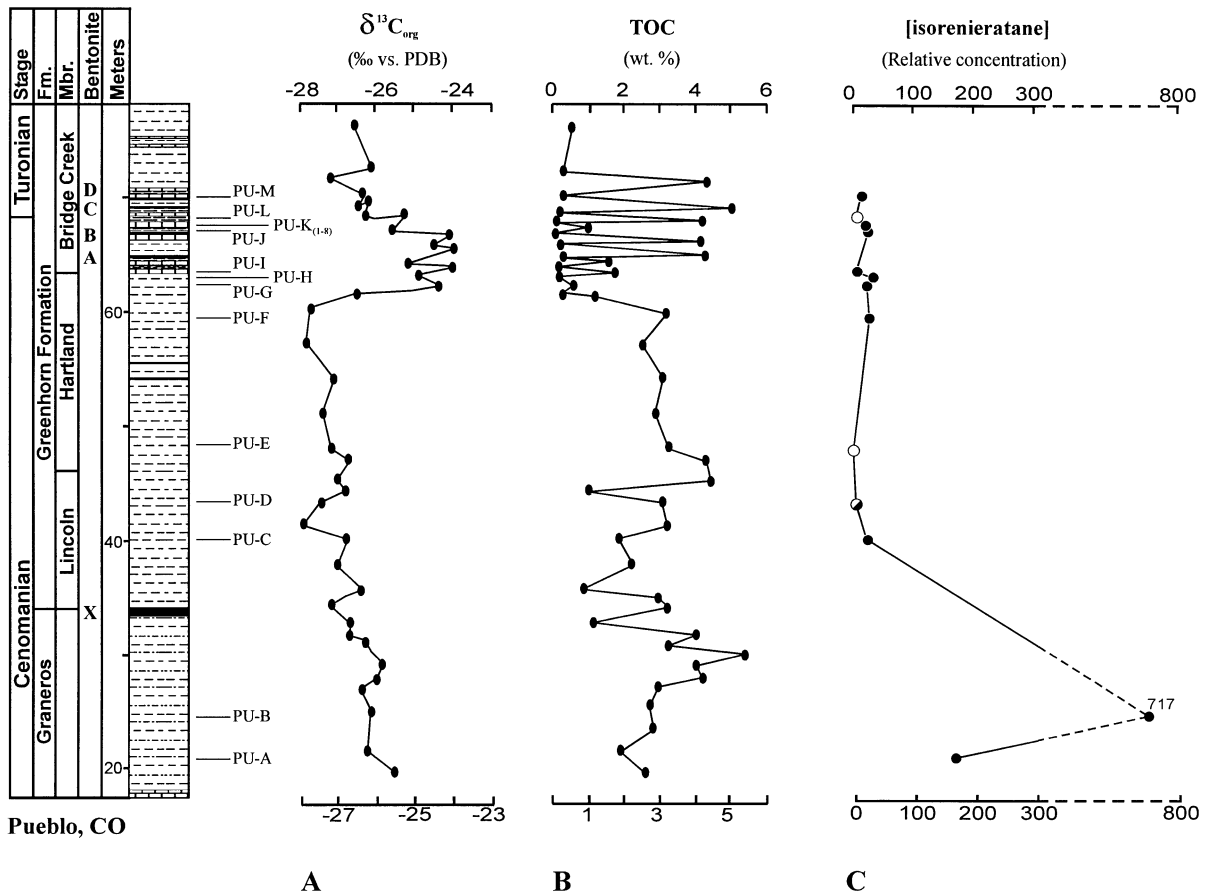


Fig. 3. Schematic stratigraphic column of the Cenomanian–Turonian outcrop at Pueblo, Colorado. (A) $\delta^{13}\text{C}_{\text{org}}$ profile (Pratt et al., 1985). Note the positive excursion at the C/T boundary. (B) TOC content (TOC, in wt.%) profile obtained from Rock–Eval analyses. (C) Relative concentration profile of isorenieratane: solid circles represent the presence of isorenieratane and aryl-isoprenoids, semi-solid circles represent the presence of aryl-isoprenoids only, and open circles indicate the absence of isorenieratene derivatives.

respectively. The TOC (wt.%) at Bunker Hill varies between 0.1 and 6.4% ($n = 54$). Shales and calcareous shales usually contain more organic carbon (0.3–6.4% TOC; $n = 29$) than carbonate rich beds ($\text{CaCO}_3 > 65\%$) which contain between 0.1 and 3.1% TOC ($n = 25$). At Pueblo, the TOC profile varies between 0.1 and 5.1% for samples with more than 65% carbonate, and varies between 0.7 and 4.8% for samples with 65% carbonate content and less. The Red Wash (RW) samples are organic-matter depleted with TOC values between 0.1 and 0.7% (average TOC of 0.5, $n = 7$; with an average carbonate content of 37.6%). Curiale (1994b) analyzed 63 samples from Red Wash and determined an average TOC of 0.7% (± 0.5 S.D.). Mueses Canyon samples are the most

organic-matter depleted with TOC content varying between 0.1 and 0.7% TOC (average TOC of 0.4, $n = 6$; with an average carbonate content of 4.7%).

At each sampling site, the TOC content profiles are highly variable but show no clear trends, other than the lower TOC values for beds with high carbonate contents. To rule out the potential effect of dilution by carbonate, TOC values were normalized to the non-carbonate component of each sample. TOC values show no significant changes: laminated shales still have higher TOC on average than limestone beds. There is a clear decrease in TOC content from east to west across the WIS. Maximum TOC values are found at Bunker Hill, whereas minimum TOC values are found in New Mexico. The observed westward

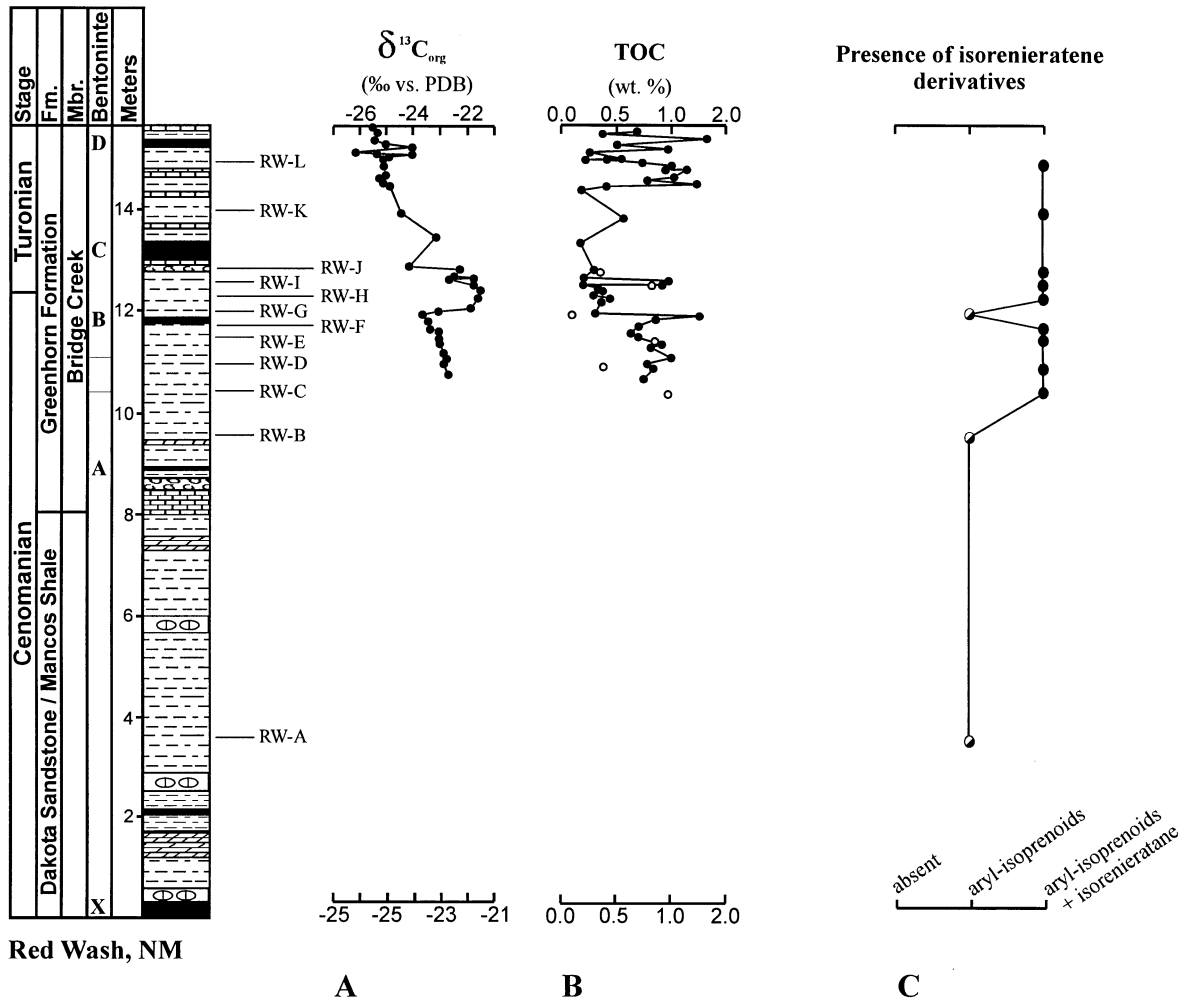


Fig. 4. Schematic stratigraphic column of the Cenomanian–Turonian outcrop at Red Wash, New Mexico. (A) $\delta^{13}C_{org}$ profile (Curiale, 1994b). Note the positive excursion at the C/T boundary. (B) TOC profile (solid circles: Curiale, 1994b; open circles: Rock–Eval analyses, this study). (C) Due to low abundance of isorenieratene derivatives, it was not possible to calculate accurate concentrations. As a consequence, only the presence of isorenieratene derivatives is indicated here: solid circles represent the presence of isorenieratene and aryl-isoprenoids, semi-solid circles represent the presence of aryl-isoprenoids only, and open circles indicate the absence of isorenieratene derivatives.

decrease in TOC content is accompanied by a westward decrease in the overall carbonate content of the sections. This is likely related to dilution by increasing terrigenous sediment input from the North American Cordillera to the West of the WIS (Kauffman and Caldwell, 1993). Consequently, sections that are more proximal to the paleo-shoreline (Red Wash and Mueses Canyon) have a higher contribution of terrigenous sediments to total deposition than sections with a more distal location (Pueblo and Bunker Hill).

4.2. Hydrogen Index, Oxygen Index, T_{max}

The plot of TOC content vs. Hydrogen index (HI, in milligram of hydrocarbon produced during pyrolysis per gram of organic carbon; Fig. 6) shows that the westward decrease in TOC content is associated by a decrease in hydrogen richness of the organic matter. Hydrogen Index is an indicator of the thermal maturation and/or of the preservation of organic matter. High values of HI (>500) are representative

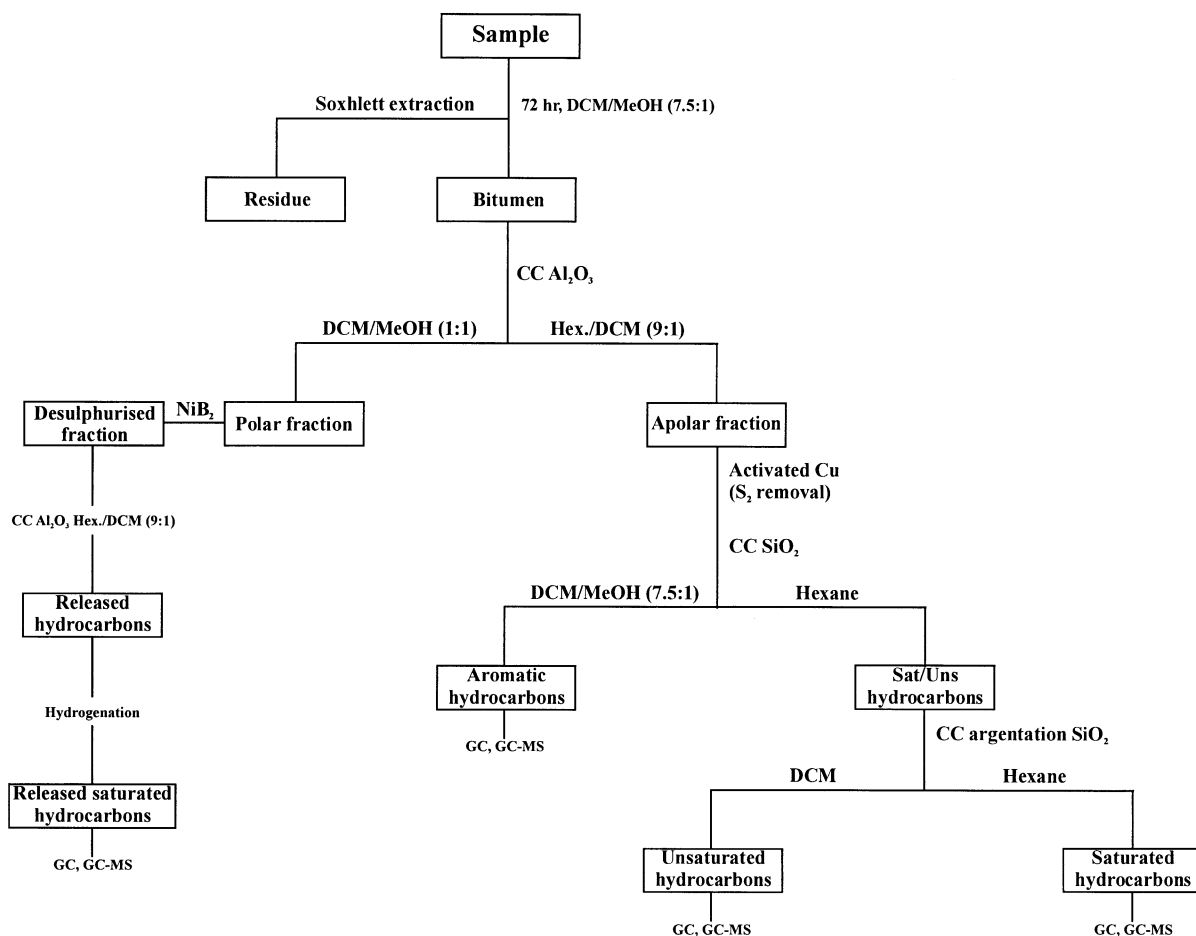


Fig. 5. Analytical flow diagram.

of well-preserved, thermally immature marine organic matter. The Oxygen Index (OI, in mg of CO₂ produced during pyrolysis per gram of organic carbon) is also obtained by Rock–Eval pyrolysis. Plots of HI vs. OI can be used as a van Krevelen-type diagram, in which H/C is plotted against O/C ratio, and identifies the type of organic matter, its thermal maturity, and its level of alteration (Fig. 7; Espitalié et al., 1977; Tissot and Welte, 1984; Kenig et al., 1994). Superimposed in Fig. 7 are evolution lines for the three main organic matter types: Type-I, bacterial, cyanobacterial, Type-II, algal marine and Type-III, terrestrial organic matter (Tissot and Welte, 1984). These lines represent pathways along which samples of a given type of organic matter will evolve as a function of increasing levels of thermal alteration

(Espitalié et al., 1977; Tissot and Welte, 1984; Hunt, 1996).

In Fig. 7, samples from Bunker Hill form a cluster between the evolution lines of Type-II and Type-III organic matter. The distribution of samples within this cluster is not following evolution lines. Hence, the spread of these data points is not the result of variation in thermal maturity, as expected given the negligible differences in burial depth of samples from this section (maximum 20 m). Pueblo, Red Wash, and Mueses Canyon samples form clusters parallel to the cluster formed by the Bunker Hill samples but with lower HI values. This gradual decrease in HI from Bunker Hill to Red Wash is likely to be associated with a westward increase in thermal maturation. This observation was confirmed with maturity parameters

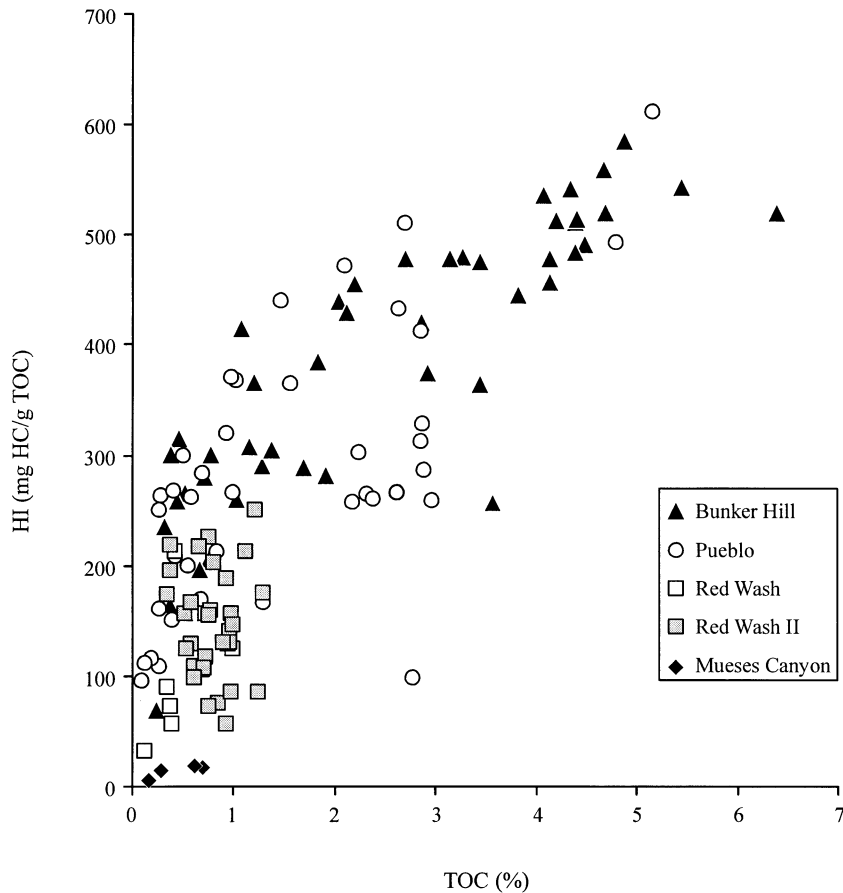


Fig. 6. Plot of TOC content (TOC, in wt%) vs. HI. Values from data set Red Wash II are taken from Curiale (1994b).

based on biomarker distributions (see below). The distribution of data points within each cluster between Type-II and Type-III organic matter can be explained by two mechanisms: (1) variable contribution of higher plant organic matter to the sediment and (2) the oxidation of marine algal organic matter during deposition and during early diagenesis (Kenig et al., 1994). In Fig. 8, samples with lower carbonate contents (<65% CaCO₃ by weight; dominated by laminated calcareous shales) plot in one distinct group with higher HI and lower OI, whereas samples with carbonate contents >65% by weight (dominated by burrowed limestone beds) plot in a region with lower HI and higher OI. For a suite of samples from Pueblo, Pratt (1984) made similar observations: on average, macro-burrowed limestone beds have low HI and high OI values, whereas finely laminated

shales are associated with high HI and low OI values. Pratt (1984) interpreted these trends as a change in redox conditions during early diagenesis: between anoxic (high HI, low OI) and more oxygenated (low HI, high OI) environments.

Mueses Canyon samples have very low HI values (Fig. 6), and plot in a cluster similar to Type-IV organic matter: organic matter deposited in oxidizing environments (Peters, 1986). Considering the proximity of Mueses Canyon to the western paleo-shoreline, these low HI and high OI values likely reflect the complete oxidative degradation of organic matter.

Rock-Eval T_{max} values do not vary significantly within each section, but do show a distinct east-west positive trend which further suggests a maturity trend observed in the HI/OI plot (Fig. 7). Bunker Hill

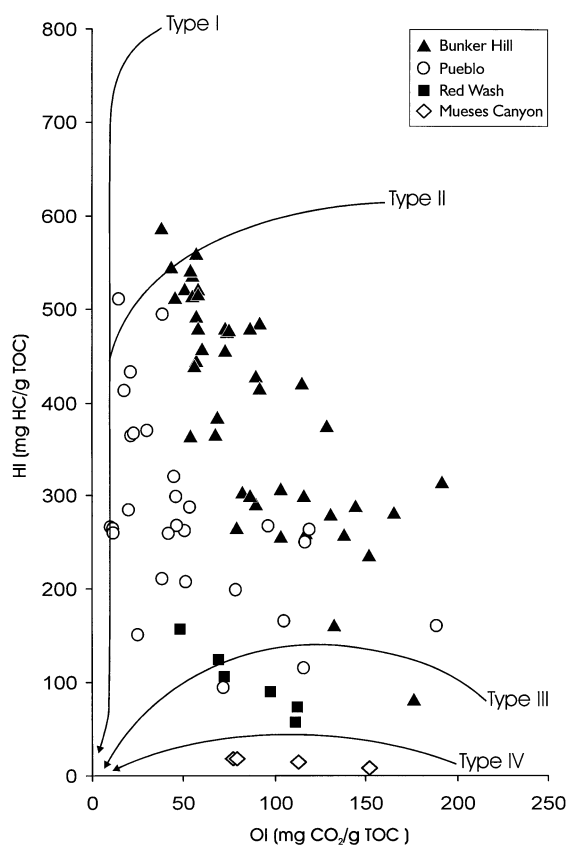


Fig. 7. Plot of oxygen index (OI) vs. HI for 81 samples from the four studied sections. Superimposed are thermal maturation evolution lines for Types I–IV organic matter.

samples have an average T_{\max} of $419 \pm 7^\circ\text{C}$ ($n = 54$), a value well below the threshold of oil generation ($\sim 435^\circ\text{C}$) for Type-II organic matter. Pueblo and Red Wash samples have distinctly higher T_{\max} values, $433 \pm 5^\circ\text{C}$ ($n = 52$) and $438 \pm 5^\circ\text{C}$ ($n = 7$) respectively, which places them just below the threshold of oil generation. Variations in T_{\max} can also be the result of changes in organic matter type (Hunt, 1996). However, biomarker maturity parameters, independent from organic matter source, confirmed the East–West maturity increase (Table 1).

Samples from the Mueses Canyon section show highest T_{\max} values with an average of $446 \pm 7^\circ\text{C}$ ($n = 6$). There are no known differences in overall burial history between Red Wash and Mueses Canyon (Wolfe, 1989). Therefore, the very high T_{\max} of Mueses Canyon samples reflect the high

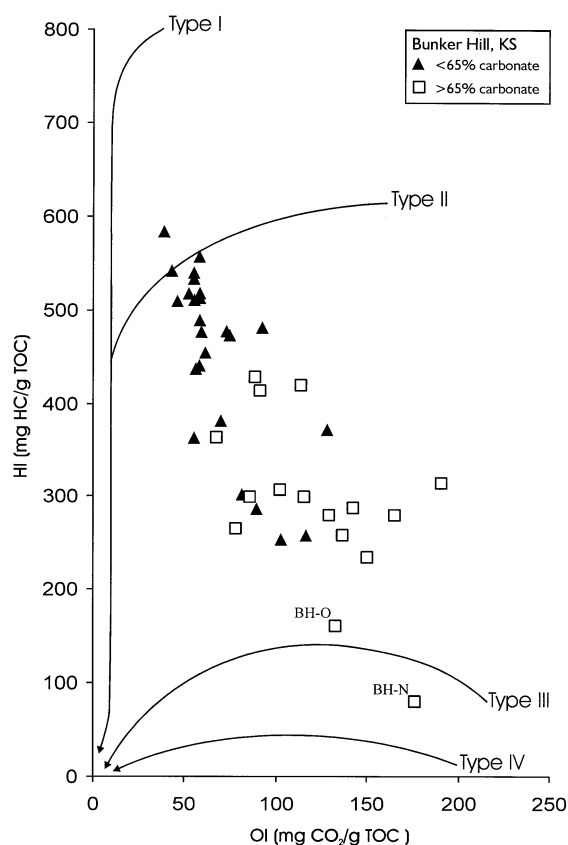


Fig. 8. Plot of oxygen index (OI) vs. HI for Bunker Hill samples as a function of carbonate carbon content.

level of organic matter degradation as observed in the HI/OI plot (Peters, 1986). Therefore, these samples were excluded from detailed biomarker analyses.

4.3. Biomarkers

4.3.1. *n*-Alkanes

The distribution of *n*-alkanes for Bunker Hill, Pueblo, and Red Wash samples varies little between samples at each site but there are differences between sites (Fig. 9). Bunker Hill samples show a bimodal distribution with a major mode centered at $n\text{-C}_{16}$ and a secondary mode centered at $n\text{-C}_{31}$. Pueblo samples have a unimodal distribution with a strong maximum at $n\text{-C}_{15}$ to $n\text{-C}_{17}$. Only one sample from Pueblo (PU-J, within the Cenomanian–Turonian boundary) has a moderate bimodal distribution, with a second mode

Table 1
Ratios of hopane stereoisomers for Bunker Hill, Pueblo and Red Wash

Hopane ratio (%)	Bunker Hill ($n = 11$)	Pueblo ($n = 7$)	Red Wash ($n = 8$)
$C_{30} - \beta\beta/(\beta\beta + \alpha\beta + \beta\alpha)$	57 ± 10	9 ± 2	10 ± 2
$C_{31} - 22S/(22S + 22R)$	19 ± 6	57 ± 1	58 ± 1
$C_{32} - 22S/(22S + 22R)$	28 ± 5	56 ± 1	57 ± 1
$C_{33} - 22S/(22S + 22R)$	22 ± 2	55 ± 2	58 ± 1

at n - C_{31} . Red Wash samples are similar to Pueblo samples and show mostly a unimodal n -alkane distribution with a maximum around n - C_{15} to n - C_{17} , although there is a weak secondary mode around n - C_{23} to n - C_{25} , and a slightly higher contribution of n - C_{29} and n - C_{31} relative to the Pueblo samples.

All samples show odd-over-even carbon predominance (OEP) in the long-chain n -alkane range (C_{27} – C_{33}). Fig. 10 shows a diagram of OEP calculated following Scalan and Smith (1970; see methods) as a function of n -alkane carbon number. Only n -alkanes with carbon number greater than 27 show a clear OEP, with a maximum between n - C_{31} and n - C_{33} . OEP values have low standard deviations, indicating that there is little variation of n -alkane distributions between samples of the same section. By far, Bunker Hill samples have the largest odd-over-even predominance as compared to the Pueblo and Red Wash sections.

4.3.2. Hopanes

Extended hopanes (C_{31} – C_{35}) found in sediments derive from bacteriohopanepolyol derivatives, lipid membrane rigidifiers in eubacteria (Ourisson et al., 1979). Hopanes are subject to irreversible changes in stereochemistry when subjected to thermal stress and can be used in the assessment of thermal maturity of organic matter (Ensminger et al., 1977; Ourisson et al., 1979; see review by Peters and Moldowan, 1993). The hopane fingerprint of immature sediments is dominated by 17β , $21\beta(H)$ biological configurations which are thermally labile and convert irreversibly to 17β , $21\alpha(H)$ - and 17α , $21\beta(H)$ configurations as a function of increasing thermal stress. The stereochemistry at the C22 chiral center in the side chain for homohopanes (extended hopanes) forms the basis for a second maturity measurement. The thermally more stable $22S$ configuration increases in abundance at the expense of the biologically derived $22R$ config-

uration, as maturity increases (Ensminger et al., 1977; Ourisson et al., 1979).

The distribution of hopane stereoisomers is used to determine levels of thermal maturity, and shows that Bunker Hill with the highest relative contribution of $\beta\beta$ -hopanes is immature. In contrast, $\alpha\beta$ -hopanes are significantly more abundant in the Pueblo and Red Wash sections, whereas $\beta\beta$ -hopanes are absent or present in low concentrations. Furthermore, the $22R$ -homohopanes are most abundant in the Bunker Hill samples compared to the Pueblo and Red Wash samples. Several maturity parameters based on hopane distribution ratios (e.g. Peters and Moldowan, 1993) confirm the difference in thermal history between the sections (Table 1). Bunker Hill strata are thermally immature, whereas Pueblo and Red Wash samples are more thermally altered but are not within the oil generating window (Mackenzie et al., 1984).

4.3.3. Aromatic hydrocarbons

The aromatic hydrocarbon fractions contain groups of aromatized steroids and hopanoids, alkyl-thiophenes, alkyl-dibenzothiophenes, and polyaromatic hydrocarbons such as alkyl-naphthalenes **II**, alkyl-phenanthrenes **III**, and alkyl-anthracenes **IV** (Fig. 11). The high relative concentration of poly-aromatic hydrocarbons in Pueblo and Red Wash samples, and the low relative concentration of these compounds in Bunker Hill samples is also an indicator of the east–west thermal maturity gradient. All samples contain benzohopanes (such as **V**; Hussler et al., 1984) with relatively higher concentrations in Pueblo and Red Wash samples. The east–west maturity trend is also visible in the differences in distribution of tri-aromatic steroids. Tri-aromatic steroids **VI** (Ludwig et al., 1981) are present in significant amounts in Pueblo and Red Wash, whereas in Bunker Hill samples tri-aromatic steroids are absent. The majority of

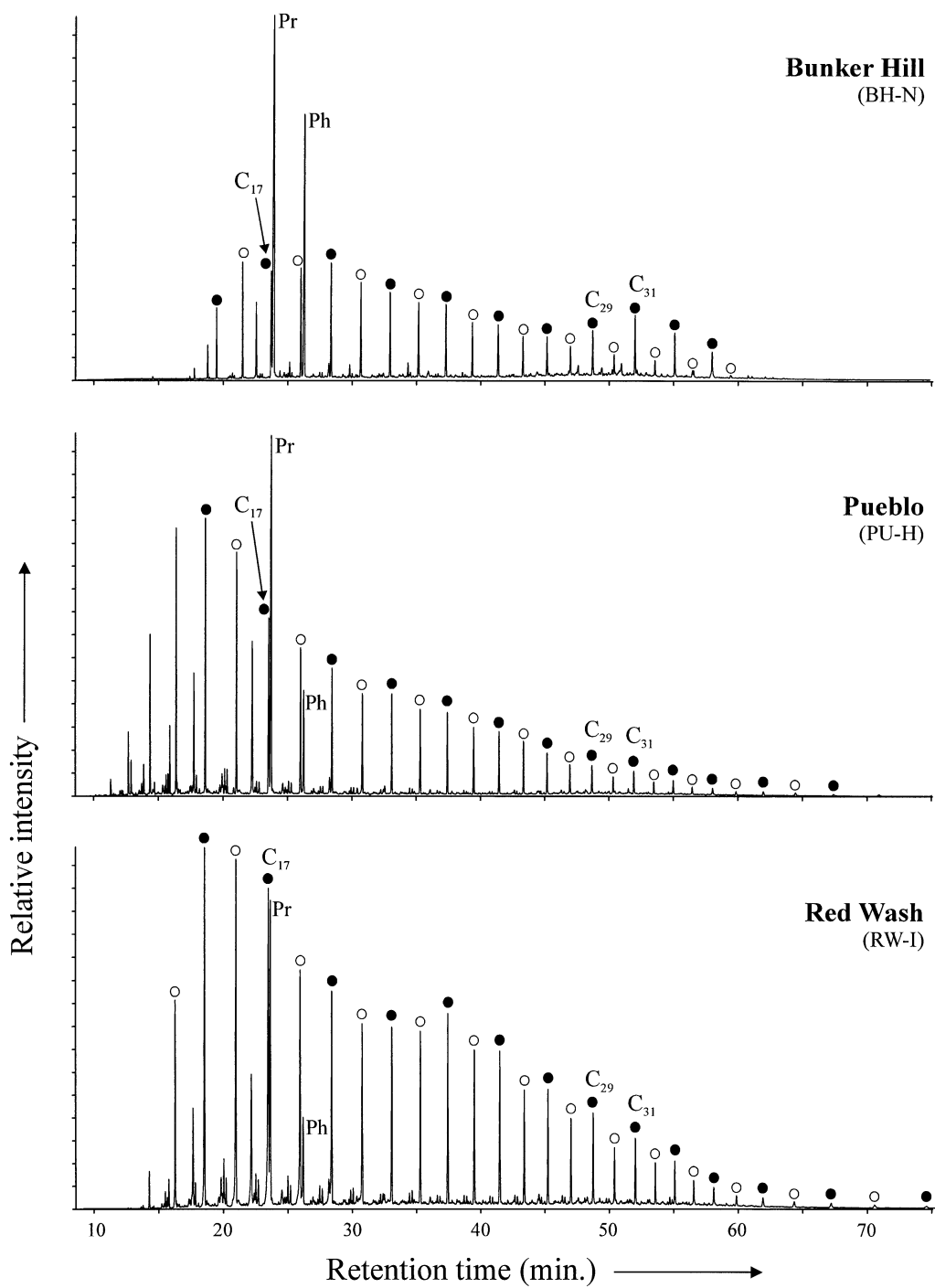


Fig. 9. Reconstructed mass chromatogram m/z 57 of the saturated hydrocarbon fraction of representative samples from Bunker Hill, Pueblo, and Red Wash. Pr and Ph indicate pristane and phytane, respectively. Solid circles represent n -alkanes with an odd number of carbon atoms, e.g. C₁₇. Open circles represent n -alkanes with an even number of carbon atoms.

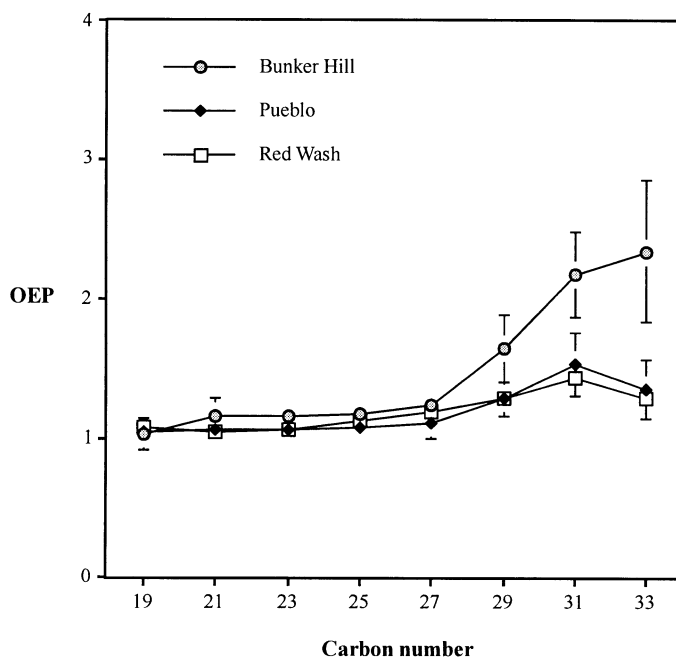


Fig. 10. Plot of odd carbon numbered *n*-alkanes versus the running odd-over-even-predominance (OEP; Scalan and Smith, 1970). *n*-Alkanes with carbon number greater than 27 have OEP values greater than 1.0, and, thus, show a predominance of odd-over-even numbered *n*-alkanes. Error bars are standard deviation of the average for $n = 10$ for Bunker Hill, $n = 8$ for Pueblo, and $n = 10$ for Red Wash.

the Bunker Hill samples contain small amounts of late eluting thienyl-hopanes **VII** (Sinninghe Damsté et al., 1989), the only sulfur bearing organic compounds present in significant quantities in all the samples analyzed. These sulfur-bearing hopanoids are not present in the Pueblo and Red Wash samples. The aromatic fractions also contain diagenetic products of isorenieratene **VIII** (Liaaen-Jensen, 1978a,b).

4.3.4. Isorenieratene and other isorenieratene derivatives

Samples from Bunker Hill, Pueblo, and Red Wash contain isorenieratene derivatives such as isorenieratane (**I**; Fig. 12), aryl-isoprenoids (**IX** and **X**) and aromatized isorenieratene derivatives (C_{32} and C_{33} , **XI–XIV**; C_{40} , **XV–XIX**). The relative distribution of isorenieratene derivatives does not vary significantly between these samples of different thermal maturity (Fig. 12).

The diaromatic carotenoid isorenieratene **VIII** is a pigment biosynthesized by the brown strain of green

sulfur bacteria *Chlorobiaceae* (Sirevåg et al., 1977). *Chlorobiaceae* are obligate anaerobic photoautotrophic organisms that require both light and H_2S . Therefore, the presence of this compound or any of its diagenetic products strongly constrains the depositional environment by imposing an anoxic water layer that reaches into the photic zone (Summons and Powell, 1986, 1987; Sinninghe Damsté et al., 1993; Kenig et al., 1995). Isorenieratene **VIII** has an irregular isoprenoid chain with a 1-alkyl-2,3,6-trimethyl substitution pattern of the aromatic rings (Liaaen-Jensen, 1978a,b; Hartgers et al., 1994). The nine sites of unsaturation make this compound susceptible to diagenetic alteration via three principal pathways (Koopmans et al., 1996a): (1) cyclization and subsequent aromatization of the isoprenoid chain, (2) release of toluene or *m*-xylene producing shorter chain compounds, and (3) reaction of isorenieratene with reduced inorganic sulfur species producing mono- and/or poly-sulfides. The products of such diagenetic reactions include C_{40} (**XV–XIX**), C_{33} and C_{32} (**XI–XIV**) and short chain aryl-isoprenoids (**IX** and **X**; Summons and Powell,

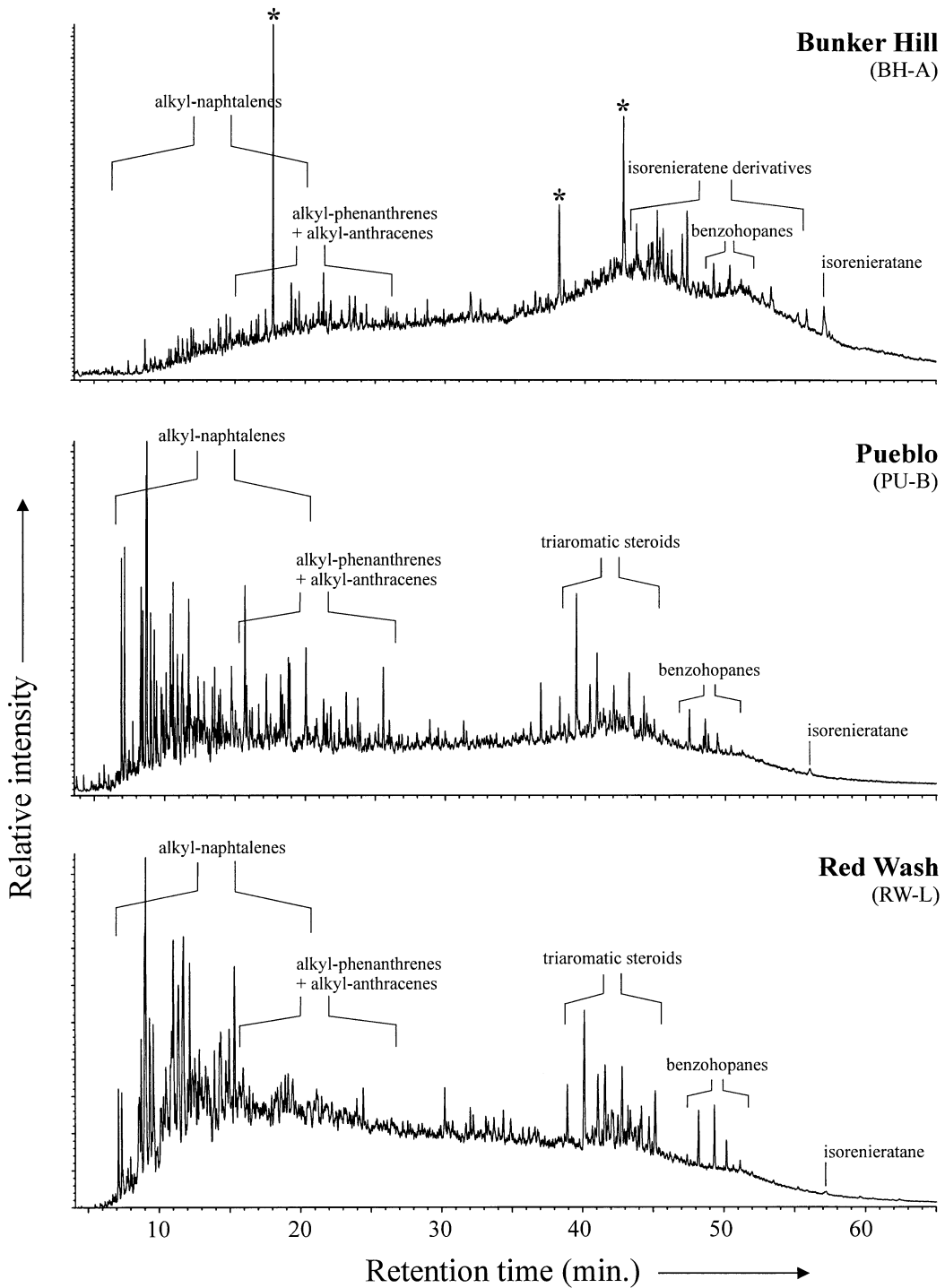


Fig. 11. Reconstructed Total Ion Current chromatogram of the aromatic fraction of three representative samples from Bunker Hill, Pueblo, and Red Wash, showing the higher abundance of polyaromatic hydrocarbons and presence of triaromatic steroids in the more mature Pueblo and Red Wash samples. Note the presence of isorenieratane I.

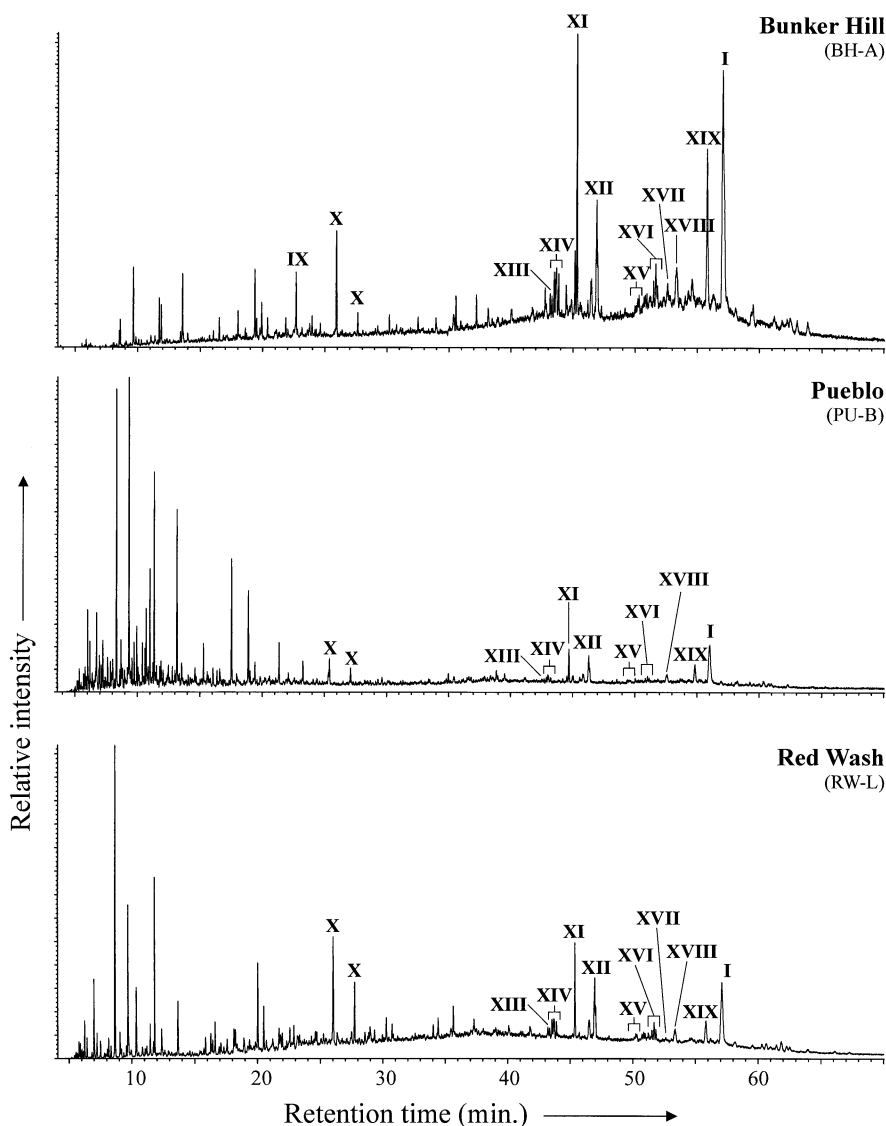


Fig. 12. Reconstructed mass chromatogram m/z 133 + 134 + 237 + 287 of the aromatic hydrocarbon fraction of representative samples from Bunker Hill, Pueblo, and Red Wash, showing the distribution of isorenieratene derivatives (isorenieratane, aromatized mono- and di-aryl-isoprenoids, and aryl-isoprenoids). Roman numbers refer to structures in Appendix A.

1987; Koopmans et al., 1996a). Koopmans et al. (1996b) discussed the limited use of aryl-isoprenoids as indicators of the presence of green sulfur bacteria, and showed that aryl-isoprenoids can be diagenetic products of β -carotene, which is not derived from *Chlorobiaceae*. However, no β -carotane is present in any of the analyzed samples. Therefore, aryl-isoprenoids detected in our samples are likely degra-

dation products of isorenieratene and can be used as indicators of photic zone anoxia.

Isorenieratene derivatives may be present in polar fractions as polysulfide bound macromolecules (Sinninghe Damsté et al., 1993; Kenig et al., 1995; Koopmans et al., 1996a). Polar fractions of 34 samples from Bunker Hill, Pueblo and Red Wash were desulfurized to release any macromolecular

bound compounds and analyzed for the presence of isorenieratene derivatives. In all desulfurized polar fractions analyzed, isorenieratane or aryl-isoprenoids were absent. Therefore, the abundance of isorenieratene derivatives, as found in the aromatic hydrocarbon fractions, represents an exact relative concentration of these compounds in the total extract.

There is a noticeable decrease in the concentration of isorenieratane in Bunker Hill samples around the Cenomanian–Turonian boundary (Fig. 2C). Furthermore, samples from the Cenomanian Graneros Shale and Turonian Jetmore member of the Greenhorn formation of Bunker Hill have the highest concentrations of isorenieratane. Similar observations are made for the Pueblo samples (Fig. 3C). Isorenieratene derivatives were considerably more abundant during deposition of the Graneros Shale and overlying Lincoln member of the Greenhorn formation, and decrease in relative concentration towards the Cenomanian–Turonian boundary (lower Bridge Creek member of the Greenhorn formation). In contrast, samples from Red Wash show a distinct opposing trend compared to the Pueblo and Bunker Hill sections (Fig. 4C). Isorenieratane and aryl-isoprenoids are absent in the Graneros- and Lincoln-equivalent Mancos Shale Fm. but are present in the Bridge Creek member, deposited during maximum transgression.

Isorenieratene derivatives were also detected in bioturbated limestone beds at Pueblo and Bunker Hill and in a burrowed shale from Bunker Hill. Fig. 13 shows a section of sample PU-K ('bed 84' in Pratt et al., 1985), a typical limestone bed of the Bridge Creek member at Pueblo, indicating distinct upward increasing levels of bioturbation. Following Savrda (1998), ichnocoenosis levels from 1–3 can be assigned to this single limestone bed. These levels of bioturbation are interpreted to correspond to variable levels of bottom water oxygenation: an ichnocoenosis 1 corresponds to "the low end of the benthic oxygenation spectrum" (dysoxic, Savrda, 1998), whereas ichnocoenosis 3 represents the highest level of benthic oxygenation (oxic). Eight sub samples from this limestone bed (PU-K_(1–8)) in Fig. 3) are analyzed for the presence of isorenieratene derivatives. Fig. 13 shows the presence of isorenieratane and aryl-isoprenoids at different intervals in PU-K. Similar observations are made for a burrowed shale–limestone bed couplet of the Lincoln Mbr. (BH–N and BH–O, Fig.

2) at Bunker Hill. The shale (BH–N)-shows burrows that correspond with ichnocoenosis 2, yet isorenieratane and aryl-isoprenoids are present in the aromatic hydrocarbon fraction. Equally, isorenieratane and aryl-isoprenoids are present in the limestone bed (BH–O), which has clear burrows that correspond to ichnocoenosis 3.

5. Discussion

5.1. Thermal maturity

Rock-Eval data show a distinct decrease in HI from Bunker Hill to Red Wash and Mueses Canyon (Figs. 6 and 7) suggesting a east–west increase in organic matter thermal maturity. This westward decrease in HI is accompanied by increasing T_{\max} values, which also suggests that samples from Bunker Hill are immature, and samples from Pueblo and Red Wash are marginally mature. The thermal maturity trend is confirmed by the hopanoid maturity parameters (Table 1). The distribution of aromatic hydrocarbons also reflects the east–west maturity trend, with a higher degree of aromatization for steroids and hopanoids at Red Wash and Pueblo than at Bunker Hill.

In summary, Rock–Eval data and an array of molecular data show that samples from Bunker Hill are immature and the Pueblo and Red Wash sections are just below the threshold of oil generation (marginally mature). Despite a Type-IV organic matter fingerprint, which is generally associated with higher T_{\max} values, Mueses Canyon samples are most likely mature. The maturity trend is the result of the burial history of the basin since Cenomanian–Turonian times. The tectonic flexure of the foreland basin gave rise to higher subsidence rates and subsequent deeper burial of Cenomanian–Turonian strata on the western margins of the Western Interior Basin (Kauffman, 1977; Armstrong and Ward, 1993). Consequently, higher degrees of thermal alteration of organic matter occurred at the western margin of the basin.

5.2. Source of extractable and bulk organic matter

Distributions of *n*-alkanes in sediments can be used to infer origin of organic matter and thermal maturity (Tissot and Welte, 1984; Collister et al., 1992; Peters

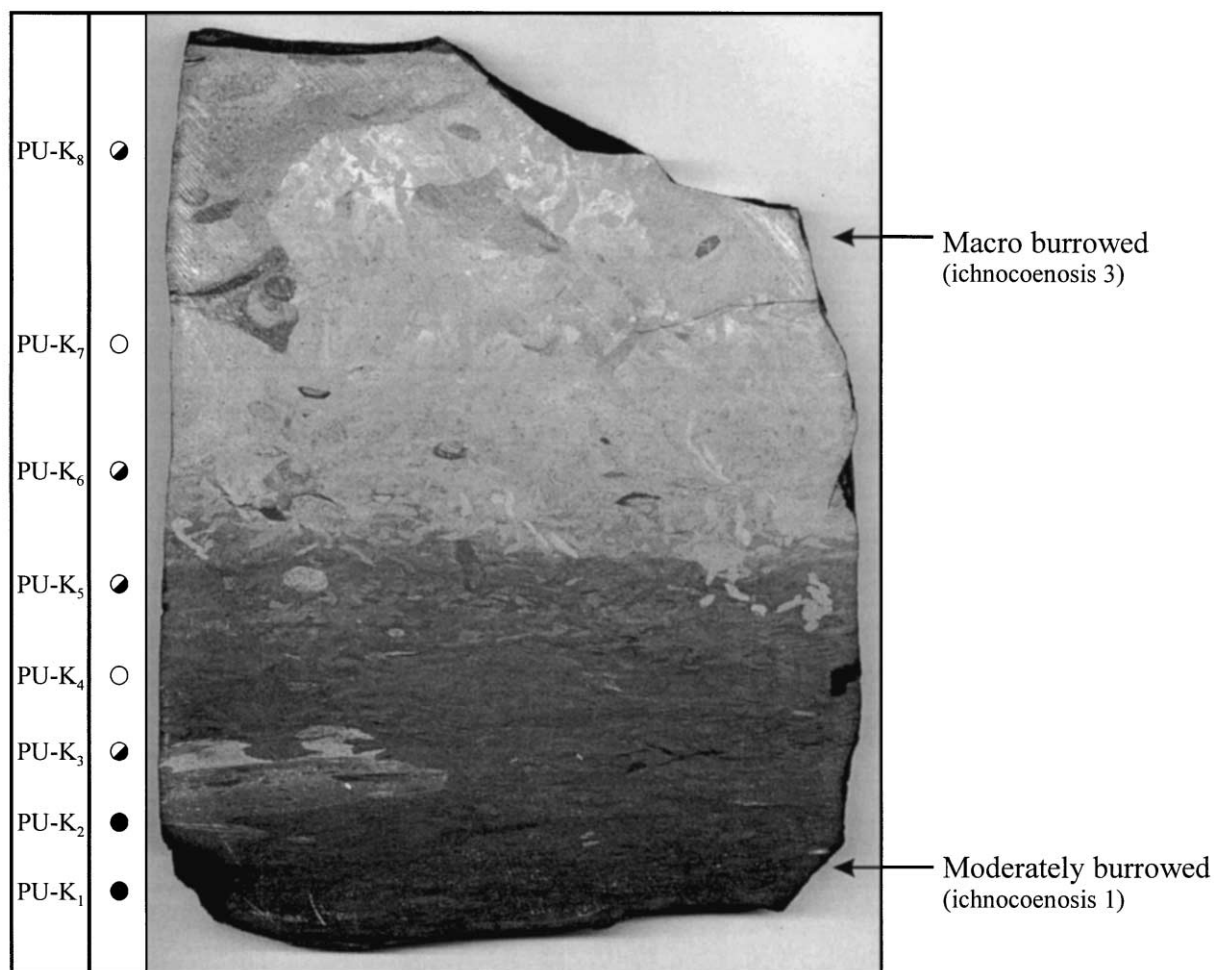


Fig. 13. Sample PU-K. Indicated on this photo are the different levels of bioturbation (ichnocoenosis 1–3), and the presence of isorenieratene derivatives in eight sub-samples. Solid circles represent the presence of isorenieratane and aryl-isoprenoids, semi-solid circles represent the presence of aryl-isoprenoids only, and open circles indicate the absence of isorenieratene derivatives.

and Moldowan, 1993). *n*-Alkanes can be divided into two groups based on their chain length: (1) short-chain alkanes with less than 19 carbon atoms, and (2) long-chain alkanes with 24 or more carbon atoms. Shorter chain *n*-alkanes, notably the *n*-C₁₇, are derived from algal and cyanobacterial precursors (e.g. Gelpi et al., 1970). The predominance of *n*-alkanes in the C₁₃–C₁₉ range (Fig. 9) indicates a dominant algal marine source of the extractable organic matter for all samples at Bunker Hill and Pueblo, but also at Red Wash. Long-chain *n*-alkanes in the C₂₃–C₃₃ range with a predominance of odd-over-even number of carbon atoms (OEP) are derived

from terrestrial plant waxes (Bray and Evans, 1961; Eglinton et al., 1962). The OEP values in the long-chain *n*-alkane range (Fig. 10) of Bunker Hill indicate a contribution from terrestrial sources for these compounds. OEP values of the Pueblo samples are very similar to the Red Wash section, and are distinctly lower than those at Bunker Hill. Scalan and Smith (1970) found that the OEP decreases with increasing thermal maturity, thus explaining the much lower OEP values of the Pueblo and Red Wash samples which are thermally more altered than those at Bunker Hill. However, since the marginally to early mature character of the Red Wash samples would

have mitigated the OEP altogether (reducing the OEP to 1.0), it is surprising to find average OEP values of up to 1.43 for these samples. The contribution of terrestrial derived plant waxes may have been relatively high at Red Wash, considering the close proximity to the paleo shoreline.

Two processes have been proposed to explain the spread of samples between Type-II and Type-III organic matter at each site: (1) a change in input of terrestrial derived organic matter or (2) a change in the redox condition of the depositional environment. The constant *n*-alkane distributions at each site (Fig. 10) suggest that the Type II–III Rock–Eval fingerprint of the organic matter of all sample sets cannot be explained by a shift in organic matter source from marine dominated to terrestrial dominated. Thus, our results do not support a change in source of organic matter, and we are now left with a change in redox condition during deposition of dominantly marine organic matter to explain the variation in HI and OI within sample sets.

5.3. Intermittent anoxia

Kenig et al. (1994, 1997) showed for the Callovian Oxford Clay formation (UK) that the changes in Rock–Eval organic matter fingerprint between Type-II and Type-III were related to differential organic matter preservation, reflecting changes in water column stratification. Extended oxic conditions of bottom water result in degradation of organic matter, indicated by a decrease in HI, and an increase in OI. Limestone and calcareous mudstone samples from Bunker Hill with relatively high carbonate contents (>65% by weight), yield lower HI and higher OI values than shale samples with lower, carbonate content (<65% by weight, Fig. 8). High carbonate contents are associated with more open marine, and well-oxygenated environments. Similar observations were made by Pratt (1984), who studied the influence of effective bottom water oxygenation on organic matter composition using Rock–Eval analyses of samples with different levels of bioturbation. This author found a distinct decrease in HI and increase in OI with higher levels of bioturbation, from laminated shales to macro-burrowed limestone beds. Therefore, the observed trends in HI and OI within sample sets (Fig. 7) are likely caused by changes in

redox conditions within the sediment during early diagenesis.

In that respect, the association of bioturbation in samples PU–K_(1–8), BH–N, and BH–O with the presence of isorenieratene derivatives is a remarkable feature. Samples BH–N and BH–O both plot close to a Type-III organic matter (Fig. 8), which suggests that these samples have been subject to higher levels of alteration. Furthermore, the observed levels of bioturbation in these samples are interpreted as indicators of oxygenated environments (Savrda, 1998). In contrast, the presence of isorenieratane and aryl-isoprenoids in these samples shows that an anoxic water column must have extended into the photic zone. Thus, our biomarker data, in conjunction with paleontologic and sedimentary features, are consistent with a scenario in which the water column experienced alternating periods of oxic/dysoxic and anoxic bottom water. Only a highly dynamic water column structure allows the deposition of single beds in which sedimentary features indicate oxic events, whereas geochemical data are consistent with anoxic events. Similarly, for the upper Jurassic Kimmeridge Clay, Wignall and Myers (1988) concluded that “relatively frequent, but brief, benthic colonization events may lead to bedding planes covered in shells in a black shale that shows the geochemical characteristics of an anaerobic deposit”, and proposed the phrase “episodically dysaerobic” for such deposits. Molecular geochemical data provided evidence for alternating oxic and anoxic events during deposition of the Kimmeridge Clay (van Kaam-Peters et al., 1997) and the Oxford Clay, (Kenig et al., 1997). These successions are referred to here as ‘intermittent anoxic events’ (Kenig et al., 1997).

In summary, the spread of samples between Type-II and Type-III organic matter in HI/OI plots (Figs. 7 and 8) indicates that the WIS experienced alternating oxic to anoxic bottom water conditions at maximum transgression. Samples plotting near Type-II are the least oxidized and represent deposition in an anoxic water column. Samples plotting near Type-III, are the most oxidized as the result of successions of anoxic and oxic/dysoxic bottom water conditions. Intermittent oxic and anoxic events, as demonstrated by bioturbated sediments containing isorenieratene derivatives, show that the change from an oxygenated water column to an anoxic water column is recurrent

within a single bed. This demonstrates that the water column structure was subject to frequent changes, illustrating the dynamic nature of the water column structure of the WIS during highstand.

5.4. History of water column stratification

The relative concentration of isorenieratane of the Bunker Hill and Pueblo sections decreases around the Cenomanian–Turonian boundary (Figs. 2 and 3). This suggests episodes of increased water column oxygenation at maximum transgression of the seaway, when the chemocline did not reach the photic zone. These distributions also show that the WIS experienced photic zone anoxia during the transgressive and regressive intervals of the Greenhorn Cyclothem at Bunker Hill and Pueblo. Not surprisingly, the highest relative concentrations of isorenieratane are associated with laminated shales in the Graneros Shale and in the lower and upper members of the Greenhorn Formation, whereas low relative concentrations or absence of isorenieratane are associated with the predominance of limestone–marly shale couplets in the Hartland Member and lower Bridge Creek Member of the Greenhorn Formation. The occurrence of “intermittent anoxic events”, during which sediments were deposited in an alternating anoxic and oxygenated environment, were rare or absent at the onset of transgression and during progressed regression, but became more common as the seaway reached maximum flooding, at which point bottom waters became more frequently oxygenated.

In contrast, isorenieratane is absent at Red Wash during the transgressive interval of the WIS and is present only at the Cenomanian–Turonian boundary during maximum transgression. This indicates that at this location, well-mixed oxygenated environments characterize the transgressive and regressive intervals of the Greenhorn Cyclothem with photic zone anoxia developing only during peak transgression. It should be noted that the Red Wash section is most proximal to the paleo-shoreline, and despite a suspected influx of fresh water at Red Wash lower sea levels probably enhanced a wind-driven mixing of the water column during initial transgression and regression and inhibited photic zone anoxia. During the sea level highstand, the deeper water column supported stratification with photic zone anoxia. In summary,

photic zone anoxia developed out of phase at Red Wash (proximal setting) compared to Pueblo and Bunker Hill (distal settings).

The increased water column oxygenation of the southern part of the WIS around the Cenomanian–Turonian boundary is also worth discussing in the light of the contemporaneous so-called C/T ‘ocean anoxic event’ (OAE; Arthur et al., 1987) of the Late Cretaceous. Two dominating operative processes can characterize the evolution of water column conditions in the WIS at the Cenomanian–Turonian boundary. One describes external environmental conditions disseminating into the WIS (e.g. Arthur et al., 1987; Glancy et al., 1993; Leckie et al., 1998). For example, Leckie et al. (1998) suggested that at maximum transgression of the Greenhorn Cyclothem, an incursion of Tethyan-derived waters imported the Tethyan OMZ into the WIS. However, the presence of abundant benthic foraminifera at the C/T boundary suggests an oxic to dysoxic benthic environment (Eicher and Worstell, 1970; Caldwell et al., 1993; Leckie et al., 1998). These inferred water column redox conditions are difficult to maintain with a maximum water depth of approximately 300 m (Kauffman, 1977). Sinninghe Damsté and Köster (1998) showed for the southern North Atlantic that photic zone anoxia was present during the C/T OAE in continental slope settings as well as in the open ocean. These authors suggested that an OMZ with ventilated (oxygenated) bottom waters did not develop in the North Atlantic, since such a scenario would facilitate organic matter destruction in the lower part of the water column and thus, would prevent the deposition of organic-rich laminated shales. These authors proposed a complete anoxic water column instead. Therefore, if an incursion of anoxic waters from the proto Gulf of Mexico and North Atlantic basin were to occur, a complete anoxic water column would have developed in the WIS at highstand, which is not supported by our results. In fact, it would impede the development and/or sustainability of a benthic community.

The generation of anoxic bottom water in the WIS, and in other contemporaneous epeiric seas, is also considered as the driving mechanism behind oceanic anoxic events, with export of anoxic water to the deeper oceanic basins (e.g. Eicher and Diner, 1989; Dean and Arthur, 1998). For such a scenario, however, an anoxic water column is required to

persist in the WIS during the OAE (at times of the maximum transgression in the WIS). Our results, associated with paleontological and sedimentological data, indicate a more complex history of bottom water redox conditions. At maximum transgression, in the WIS, the co-occurrence of burrows and isorenieratene derivatives in limestone beds and shales indicates that bottom water anoxia alternated with periods of bottom water oxygenation. On the contrary, laminated shales deposited during the transgression (Graneros Shale and lower shales of the Lincoln member) and the regression (shales from the Jetmore member) of the Greenhorn Cyclothem contain isorenieratane and, thus, were likely deposited under a permanently stratified water mass with anoxic bottom water. Thus, oxic–anoxic bottom water successions in the WIS functioned independently from proto-Atlantic oceanic forcing. The positive $\delta^{13}\text{C}$ excursion of carbonate and TOC around the Cenomanian–Turonian of the WIS (e.g. Figs. 2A, 3A and 4A; Pratt, 1985; Curiale, 1994b) reflect changes in the isotopic composition of atmospheric CO_2 induced by burial of ^{13}C depleted organic carbon during the OAE (Arthur et al., 1988). Hence, our results suggest that organic matter burial in the WIS during deposition of the Greenhorn Cyclothem recorded, but was not directly influenced by, the contemporaneous proto-Atlantic OAE.

Paleoceanographic models based on atmospheric circulation lack sufficient spatial and temporal resolution to generate insights on water column conditions and subsequent impact on the paleoceanography of the WIS (Kump and Slingerland, 1999). Our results indicate that stratification with bottom water anoxia was a dominant but not continuous feature of the southern part of the WIS during deposition of the Greenhorn Cyclothem, providing new boundary conditions for evolving oceanographic models of Cretaceous epicontinental seaways. The oceanographic causes of anoxia and intermittent anoxia during deposition of the Greenhorn Cyclothem are inherent to the WIS, but remain unclear.

6. Conclusions

Rock–Eval pyrolyses and biomarker analyses reveal trends in thermal maturity and source of organic matter. Bunker Hill samples are immature, and Pueblo and Red

Wash samples are early mature, following an east–west trend of deeper burial history. This westward increase in thermal maturity is associated with the tectonic flexure of the foreland basin, which resulted in higher subsidence rates and subsequent deeper burial of Cenomanian–Turonian strata on the western margins of the Western Interior Basin. The source of organic matter is dominantly marine with the exception of samples from Mueses Canyon, which have a distinct Type-IV kerogen fingerprint.

The presence of isorenieratene derivatives in samples from Bunker Hill, Pueblo, and Red Wash indicates that the southern part of the WIS experienced events of photic zone anoxia. At maximum transgression, sedimentary features indicative of water column oxygenation (bioturbation and fossil assemblage) occur within single beds with geochemical evidence of photic zone anoxia (isorenieratene derivatives). These so-called ‘intermittent anoxic events’ underline the high variability in redox conditions in the WIS. Hence, combined paleoenvironmental assessment using the molecular fossil record associated with paleontologic and sedimentary data provides strong constraints for paleoceanographic reconstruction.

The distribution of isorenieratene derivatives shows a dynamic water column structure of the WIS during the Greenhorn Cyclothem. A stratified water column with bottom water anoxia reaching into the photic zone was especially prominent during transgression and late regression at Bunker Hill and Pueblo, and during highstand at Red Wash. At maximum transgression, oxygenated bottom water conditions alternated with intermittent anoxic events in the WIS.

The maximum extent of anoxic events in the WIS did not correspond with the Cenomanian–Turonian Oceanic Anoxic Event. Therefore, the oceanographic circulation is dominated by near field effects inherent to the seaway, rather than by direct proto-Atlantic influences.

Acknowledgements

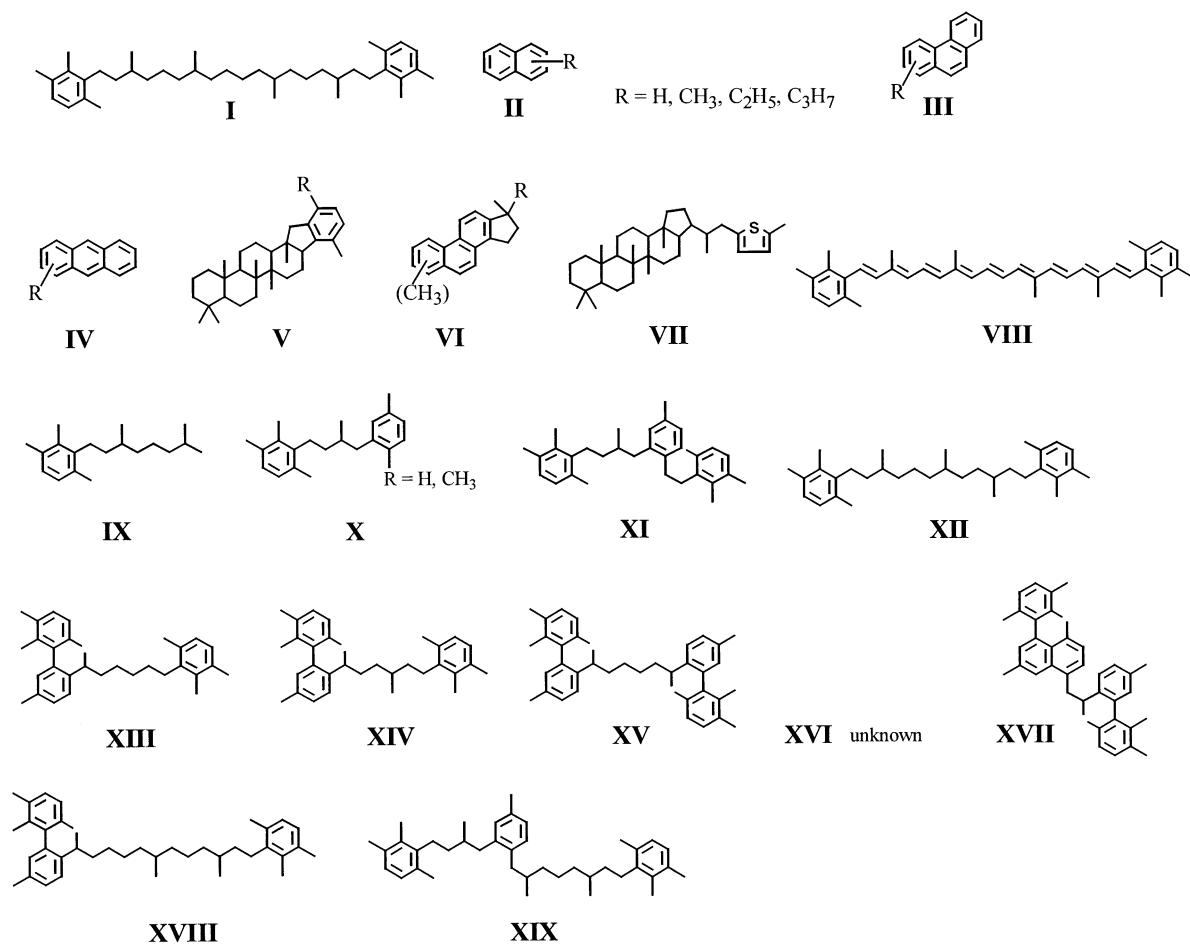
The research was supported by NSF grant EAR-9614769 to F.K. The authors wish to thank Erle Kauffman for help with fieldtrip organization and

good advise at the onset of this project. Doug Wolfe and Will Elder are thanked for their help as field guides in New Mexico and Arizona. Robert Hoback (Russell County Highway Department), the Navajo Nation Minerals Department, the Park District of the City of Pueblo, CO, and the Lake Pueblo State Park administration are thanked for granting permission to sample. Eric Lafargue and Alain Y. Huc (Institut Français du Pétrole) are thanked for Rock–Eval analyses. J.S. Sinninghe Damsté and W.E. Dean are thanked for providing constructive reviews on an earlier draft of this manuscript.

References

- Armstrong, R.L., Ward, P., 1993. Late Triassic to Earliest Miocene magmatism in the North American Cordillera: implications for the Western Interior Basin. *Evolution of the Western Interior Basin*, Caldwell, W.G.E., Kauffman, E.G. (Eds.). Geol. Assoc. Can. Spec. Pap. 39, 49–72.
- Arthur, M.A., Schlanger, S.O., Jenkyns, H.C., 1987. The Cenomanian–Turonian oceanic anoxic event, II. Paleoclimatographic controls on organic matter production and preservation. *Marine Petroleum Source Rocks*, Brooks, J., Fleet, A. (Eds.). Geol. Soc. Lond. Spec. Publ. 26, 401–420.
- Arthur, M.A., Dean, W.E., Pratt, L.M., 1988. Geochemical and climatic effects of increased organic carbon burial at the Cenomanian/Turonian boundary. *Nature* 335, 714–717.

Appendix A



- Bralower, T.J., 1988. Calcareous nannofossil biostratigraphy and assemblages of the Cenomanian–Turonian boundary interval: implications for the origin and timing of oceanic anoxia. *Paleoceanography* 3, 275–316.
- Bray, E.E., Evans, E.D., 1961. Distribution of *n*-paraffins as a clue to the recognition of source beds. *Geochim. Cosmochim. Acta* 22, 2–9.
- Caldwell, W.G.E., Kauffman, E.G., 1993. Evolution of the Western Interior Basin. *Geol. Assoc. Can. Spec. Pap.*, 39.
- Caldwell, W.G.E., Diner, R., Eicher, D.L., Fowler, S.P., North, B.R., Stelck, C.R., von Holdt Wilholm, L., 1993. Foraminiferal biostratigraphy of Cretaceous marine cyclothem. Evolution of the Western Interior Basin, Caldwell, W.G.E., Kauffman, E.G. (Eds.). *Geol. Assoc. Can. Spec. Pap.* 39, 477–521.
- Cobban, W.A., 1993. Diversity and Distribution of late Cretaceous Ammonites, Western Interior, United States. Evolution of the Western Interior Basin, Caldwell, W.G.E., Kauffman, E.G. (Eds.). *Geol. Assoc. Can. Spec. Pap.* 39, 435–452.
- Collister, J.W., Summons, R.E., Lichtfouse, E., Hayes, J., 1992. An isotopic biogeochemical study of the Green River oil shale. *Org. Geochem.* 19, 265–276.
- Curiale, J.A., 1994a. High-resolution organic record of Bridge Creek deposition, northwest New Mexico. *Org. Geochem.* 21, 489–507.
- Curiale, J.A., 1994b. Geochemical anomalies at the Cenomanian–Turonian boundary, northwest New Mexico. *Org. Geochem.* 22, 487–500.
- Dean, W.A., Arthur, M.A., 1998. Cretaceous Western Interior Seaway drilling project: an overview. Stratigraphy and Paleoenvironments of the Cretaceous Western Interior Seaway, USA, Dean, W.A., Arthur, M.A. (Eds.). *SEPM Concepts Sedimentol. Paleontol.* 6, 1–10.
- Eglinton, G., Gonzalez, A.G., Hamilton, R.J., Raphael, R.A., 1962. Hydrocarbon constituents of wax coatings of plant leaves: a taxonomic survey. *Phytochemistry* 1, 89–102.
- Eicher, D.L., Diner, R., 1985. Foraminifera as indicators of water mass in the Cretaceous Greenhorn Sea, Western Interior. In: Pratt, L.M., Kauffman, E.G., Zelt, F.B. (Eds.), *Fine-grained Deposits and Biofacies of the Cretaceous Western Interior Seaway: Evidence of Cyclic Sedimentary Processes: Evidence of Cyclic Sedimentary Processes*. *SEPM Field Trip Guidebook*, vol. 4, pp. 60–71.
- Eicher, D.L., Diner, R., 1989. Origin of the Cretaceous Bridge Creek cycles in the Western Interior, United States. *Palaeogeogr., Palaeoclimatol., Palaeoecol.* 74, 127–146.
- Eicher, D.L., Worstell, P., 1970. Cenomanian and Turonian foraminifera from the Great Plains, United States. *Micropaleontology* 16 (3), 269–324.
- Elder, W.P., 1985. Biotic patterns across the Cenomanian–Turonian boundary near Pueblo, Colorado. In: Pratt, L.M., Kauffman, E.G., Zelt, F.B. (Eds.), *Fine-grained Deposits and Biofacies of the Cretaceous Western Interior Seaway: Evidence of Cyclic Sedimentary Processes*. *SEPM Field Trip Guidebook*, vol. 4, pp. 157–169.
- Elder, W.P., 1987. The paleoecology of the Cenomanian–Turonian (Cretaceous) stage boundary extinctions at Black Mesa, Arizona. *Palaios* 2, 157–169.
- Elder, W.P., 1991. Molluscan paleoecology and sedimentation patterns of the Cenomanian–Turonian extinction interval in the southern Colorado Plateau region. Stratigraphy, depositional environment, and sedimentary tectonics of the Western Margin, Cretaceous Western Interior Seaway, Nations, J.D., Eaton, J.G. (Eds.). *Geol. Soc. Am. Spec. Pap.* 260, 113–137.
- Elder, W.P., Kirkland, J.L., 1985. Stratigraphy and depositional environments of the Bridge Creek Limestone Member of the Greenhorn Formation at Rock Canyon Anticline near Pueblo, Colorado. In: Pratt, L.M., Kauffman, E.G., Zelt, F.B. (Eds.), *Fine-grained Deposits and Biofacies of the Cretaceous Western Interior Seaway: Evidence of Cyclic Sedimentary Processes*. *SEPM Field Trip Guidebook*, vol. 4, pp. 122–134.
- Elder, W.P., Gustason, E.R., Sageman, B.B., 1994. Correlation of basinal carbonate cycles to nearshore parasequences in the late Cretaceous Greenhorn Seaway, Western Interior USA. *Geol. Soc. Am. Bull.* 106, 892–902.
- Ensminger, A., Albrecht, P., Ourisson, G., Tissot, B., 1977. Evolution of polycyclic alkanes under the effect of burial (Early Toarcian shales, Paris Basin). In: Campos, R., Goni, J. (Eds.), *Advances in Organic Geochemistry 1975*. *ENADIMSA, Madrid*, pp. 45–52.
- Ericksen, M.C., Slingerland, R.L., 1990. Numerical simulations of tidal and wind-driven circulation in the Cretaceous Interior Seaway of North America. *Geol. Soc. Am. Bull.* 102, 1499–1516.
- Espitalié, J., Laporte, J.L., Madec, M., Marquis, F., Leplat, P., Paulet, J., 1977. Méthode rapide de caractérisation des roches mères, de leur potentiel pétrolier et de leur degré d'évolution. *Revue de l'Institut Français du Pétrole* 32, 23–45.
- Frush, M.P., Eicher, D.L., 1975. Cenomanian and Turonian foraminifera and paleoenvironments in the Big Bend region in Texas and Mexico. The Cretaceous System in the Western Interior of North America, Caldwell, W.G.E. (Ed.). *Geol. Assoc. Can. Spec. Pap.* 13, 277–301.
- Gelpi, E., Schneider, H., Mann, J., Oro, J., 1970. Hydrocarbons of geochemical significance in microscopic algae. *Phytochemistry* 9, 603–612.
- Glancy, T.J., Arthur, M.A., Barron, E.J., Kauffman, E.G., 1993. A paleoclimate model for the North American Cretaceous (Cenomanian–Turonian) Epicontinental Sea. Evolution of the Western Interior Basin, Caldwell, W.G.E., Kauffman, E.G. (Eds.). *Geol. Assoc. Can. Spec. Pap.* 39, 219–242.
- Hancock, J.M., Kauffman, E.G., 1979. The Great Transgressions of the late Cretaceous. *J. Geol. Soc. Lond.* 136, 175–186.
- Hartgers, W.A., Sinninghe Damsté, J.S., Requejo, A.G., Allan, J., Hayes, J.M., Yue, L., Xie, T.-M., Primack, J., de Leeuw, J.W., 1994. A molecular and carbon isotopic study towards the origin and diagenetic fate of diaromatic carotenoids. *Org. Geochem.* 22, 703–725.
- Hattin, D.E., 1965. Stratigraphy of the Graneros Shale (Upper Cretaceous) in Central Kansas. *State Geol. Surv. Kansas Bull.* 178, 5–83.
- Hattin, D.E., 1975. Stratigraphy and Depositional Environment of Greenhorn Limestone (Upper Cretaceous) of Kansas. *State Geol. Surv. Kansas Bull.* 209, 14–105.
- Hay, W.W., Eicher, D.L., Diner, R., 1993. Physical Oceanography and Water Masses in the Cretaceous Western Interior Seaway.

- The Cretaceous System in the Western Interior of North America, Caldwell, W.G.E., Kauffman, E.G. (Eds.). *Geol. Assoc. Can. Spec. Pap.* 13, 297–318.
- Hayes, J.M., Popp, B.N., Takigiku, R., Johnson, M.W., 1989. An isotopic study of biogeochemical relationships between carbonates and organic carbon in the Greenhorn Formation. *Geochim. Cosmochim. Acta* 53, 2961–2972.
- Hunt, J.M., 1996. *Petroleum Geochemistry and Geology*. 2nd ed. W.H. Freeman and Company, New York.
- Hussler, G., Connan, J., Albrecht, P., 1984. Novel families of tetra- and hexacyclic aromatic hopanoids predominant in carbonate rocks and oils. *Org. Geochem.* 6, 39–49.
- van Kaam-Peters, H.M.E., Schouten, S., de Leeuw, J.W., Sinninghe Damsté, J.S., 1997. A molecular and carbon isotope biogeochemical study of biomarkers and kerogen pyrolysates of the Kimmeridge Clay Facies: palaeoenvironmental implications. *Org. Geochem.* 27 (7–8), 399–422.
- Kauffman, E.G., 1973. In: Hallam, A. (Ed.). *Atlas of Paleobiogeography*. Elsevier, Amsterdam, pp. 353–383.
- Kauffman, E.G., 1975. Dispersal and biostratigraphic potential of Cretaceous benthonic Bivalvia in the Western Interior. *The Cretaceous System in the Western Interior of North America*, Caldwell, W.G.E., Kauffman, E.G. (Eds.). *Geol. Assoc. Can. Spec. Pap.* 13, 163–194.
- Kauffman, E.G., 1977. Geological and biological overview: Western Interior Cretaceous Basin. *Mountain Geologist* 14, 75–99.
- Kauffman, E.G., 1984. Paleobiogeography and evolutionary response dynamic in the Cretaceous Western Interior seaway of North America. *Jurassic–Cretaceous Biochronology and Paleogeography of North America*, Westerman, G.E.G. (Ed.). *Geol. Assoc. Can. Spec. Pap.* 27, 273–306.
- Kauffman, E.G., Caldwell, W.G.E., 1993. The Western Interior Basin in space and time. *Evolution of the Western Interior Basin*, Caldwell, W.G.E., Kauffman, E.G. (Eds.). *Geol. Assoc. Can. Spec. Pap.* 39, 1–30.
- Kauffman, E.G., Sageman, B.B., 1990. Biological sensing of benthic environments in dark shale and related oxygen restricted facies. In: Ginsburg, R.N., Beaudoin, B. (Eds.), *Cretaceous Resources, Events and Rhythms*. Kluwer, Amsterdam, pp. 121–138.
- Kenig, F., Hayes, J.M., Popp, B.N., Summons, R.E., 1994. Isotopic biogeochemistry of the Oxford Clay Formation (Jurassic), UK. *J. Geol. Soc. Lond.* 151, 139–152.
- Kenig, F., Sinninghe Damsté, J.S., Frewin, N.L., Hayes, J.M., de Leeuw, J.W., 1995. Molecular indicators for palaeoenvironmental change in a Messinian evaporitic sequence (Vena del Gesso, Italy); II, High-resolution variations in abundances and ^{13}C contents of free and sulfur-bound carbon skeletons in a single marl bed. *Org. Geochem.* 23, 485–526.
- Kenig, F., Popp, B.N., Sinninghe Damsté, J.S., 1997. Intermittent Anoxia: a process that reunites Black Shales and their biofacies, GSA Abstracts, 1997 GSA Annual Meeting, Salt Lake City, p. 108.
- Koopmans, M.P., Köster, J., van Kaam-Peters, H.M.E., Kenig, F., Schouten, S., Hartgers, W.A., de Leeuw, J.W., Sinninghe Damsté, J.S., 1996a. Diagenetic and catagenetic products of isorenieratene; molecular indicators for photic zone anoxia. *Geochim. Cosmochim. Acta* 60, 4467–4496.
- Koopmans, M.P., Schouten, S., Köhnen, M.E.L., Sinninghe Damsté, J.S., 1996b. Restricted utility of aryl isoprenoid as indicators of photic zone anoxia. *Geochim. Cosmochim. Acta* 60, 4873–4876.
- Kump, L.R., Slingerland, R.L., 1999. Circulation and stratification of the early Turonian Western Interior Seaway: Sensitivity to a variety of forcings. *Evolution of the Cretaceous Ocean-Climate System*, Barrera, E., Johnson, C.C. (Eds.). *Geol. Soc. Am. Spec. Pap.* 332, 181–191.
- Lafargue, E., Marquis, F., Pillot, D., Bernard, M., Beauducel, G., Antonas, R., Burwood, R., 1997. Rock Eval 6: a new generation of Rock Eval pyrolyser for a wider use in petroleum exploration/production and in soil contamination studies. *AAPG International Conference and Exhibition, abstracts*, AAPG Bull 81, p. 1393.
- Leckie, R.M., 1985. Foraminifera of the Cenomanian–Turonian boundary interval, Greenhorn Formation, Rock Canyon Anticline, Pueblo, Colorado. In: Pratt, L.M., Kauffman, E.G., Zelt, F.B. (Eds.), *Fine-grained Deposits and Biofacies of the Cretaceous Western Interior Seaway: Evidence of Cyclic Sedimentary Processes*. SEPM Field Trip Guidebook, vol. 4, pp. 139–149.
- Leckie, R.M., Schmidt, M.G., Finkelstein, D., Yuretich, R.F., 1991. Paleocceanographic and paleoclimatic interpretation of the Mancos Shale (Upper Cretaceous), Black Mesa Basin, Arizona. *Stratigraphy, depositional environment, and sedimentary tectonics of the Western Margin, Cretaceous Western Interior Seaway*, Nations, J.D., Eaton, J.G. (Eds.). *Geol. Soc. Am. Spec. Pap.* 260, 139–152.
- Leckie, R.M., Yuretich, R.F., West, O.L.O., Finkelstein, D., Schmidt, M., 1998. Paleocceanography of the southwestern Western Interior Sea during the time of the Cenomanian–Turonian boundary (Late Cretaceous). *Stratigraphy and Paleoenvironments of the Cretaceous Western Interior Seaway, USA*, Dean, W.A., Arthur, M.A. (Eds.). *SEPM Concepts Sedimentol. Paleontol.* 6, 101–126.
- Liaaen-Jensen, S., 1978a. Chemistry of carotenoid pigments. In: Clayton, R.K., Sistrom, W.R. (Eds.), *The Photosynthetic Bacteria*. Plenum Press, New York, pp. 233–247.
- Liaaen-Jensen, S., 1978b. Marine carotenoids. In: Faulkner, D.J., Fenical, W.H. (Eds.), *Marine Natural Products*. Academic Press, New York, pp. 1–73.
- Ludwig, B., Hussler, G., Wehrung, P., Albrecht, P., 1981. C₂₆–C₂₉ triaromatic steroid derivatives in sediments and petroleum. *Tetrahedron Lett.* 22 (34), 3313–3316.
- Mackenzie, A.S., Maxwell, J.R., Coleman, M.L., Deegan, C.E., 1984. Biological Marker and Isotope Studies of North Sea Crude Oils and Sediments. *Proceedings of the 11th World Petroleum Congress*, vol. 2. Wiley, New York, pp. 45–56.
- Mieras, B.L., Sageman, B.B., Kauffman, E.G., 1993. Trace Fossil Distribution Patterns in Cretaceous Facies of the Western Interior Basin, North America. *Evolution of the Western Interior Basin*, Caldwell, W.G.E., Kauffman, E.G. (Eds.). *Geol. Assoc. Can. Spec. Pap.* 39, 585–621.

- Molenaar, C.M., 1977. Stratigraphy and depositional history of upper Cretaceous rocks of the San Juan Basin area, New Mexico and Colorado, with a note on economic resources. In: Fassett, J.E. (Ed.). San Juan basin III, New Mexico Geological Society Guidebook, 28th Field Conference, pp. 159–166.
- Monger, J.W.H., 1993. Cretaceous Tectonics of the North American Cordillera. Evolution of the Western Interior Basin, Caldwell, W.G.E., Kauffman, E.G. (Eds.). Geol. Assoc. Can. Spec. Pap. 39, 31–47.
- Ouirsson, G., Albrecht, P., Rohmer, M., 1979. The hopanoids: palaeochemistry and biochemistry of a group of natural products. *Pure Appl. Chem.* 51, 709–729.
- Peters, K.E., 1986. Guidelines for evaluating petroleum source rock using programmed pyrolysis. *AAPG Bull.* 70, 318–329.
- Peters, K., Moldowan, J., 1993. *The Biomarker Guide: Interpreting Molecular Fossils in Petroleum and Ancient Sediments*. Prentice Hall, Englewood Cliffs, New Jersey.
- Pratt, L.M., 1984. Influence of paleoenvironmental factors on preservation of organic matter in middle Cretaceous Greenhorn formation, Pueblo, Colorado. *AAPG Bull.* 68, 1146–1159.
- Pratt, L.M., 1985. Isotopic studies of organic matter and carbonate in rocks of the Greenhorn marine cycle. In: Pratt, L.M., Kauffman, E.G., Zelt, F.B. (Eds.), *Fine-grained Deposits and Biofacies of the Cretaceous Western Interior Seaway: Evidence of Cyclic Sedimentary Processes*. SEPM Field Trip Guidebook, vol. 4, pp. 38–48.
- Pratt, L.M., Kauffman, E.G., Zelt, F.B., 1985. *Fine-grained Deposits and Biofacies of the Cretaceous Western Interior Seaway: Evidence of Cyclic Sedimentary Processes*. SEPM Field Trip Guidebook, vol. 4, pp. 60–71.
- Reyment, R.A., 1980. Biogeography of Saharan Cretaceous and Paleocene epicontinental transgressions. *Cretaceous Res.* 1, 299–327.
- Sageman, B.B., Wignall, P.B., Kauffman, E.G., 1991. Biofacies models for oxygen deficient facies in epicontinental seas: tools for paleoenvironmental analysis. In: Einsele, G., Ricken, W., Seilacher, A. (Eds.), *Cycles and Events in Stratigraphy*. Springer, Berlin, pp. 542–564.
- Savrdra, C.E., 1998. Technology of the Bridge Creek Limestone: Evidence for temporal and spatial variations in paleo-oxygenation in the Western Interior Seaway. *Stratigraphy and Paleoenvironments of the Cretaceous Western Interior Seaway, USA*, Dean, W.A., Arthur, M.A. (Eds.). SEPM Concepts Sedimentol. Paleontol. 6, 127–136.
- Savrdra, C.E., Bottjer, D.J., 1993. Trace Fossil Assemblages in Fine-grained Strata of the Cretaceous Western Interior. Evolution of the Western Interior Basin, Caldwell, W.G.E., Kauffman, E.G. (Eds.). Geol. Assoc. Can. Spec. Pap. 39, 621–640.
- Scalan, R.S., Smith, J.E., 1970. An improved measure of the odd–even predominance in the normal alkanes of sediment extracts and petroleum. *Geochim. Cosmochim. Acta* 34, 611–620.
- Schaeffe, J., Ludwig, B., Albrecht, P., Ouirsson, G., 1977. Hydrocarbures aromatiques d'origine geologique: nouveaux carénoïdes aromatiques fossiles. *Tetrahedron Lett.* 41, 3673–3676.
- Schlanger, S.O., Jenkyns, H.C., 1976. Cretaceous oceanic anoxic events: causes and consequences. *Geol. Mijnbouw* 55, 179–184.
- Schlanger, S.O., Arthur, M.A., Jenkyns, H.C., Scholle, P.A., 1987. The Cenomanian–Turonian oceanic anoxic event. I. Stratigraphy and distribution of organic carbon-rich beds and the marine C excursion. *Marine Petroleum Source Rocks*, Brooks, J., Fleet, A.J. (Eds.). Geol. Soc. Lond. Spec. Publ. 26, 371–399.
- Schouten, S., Pavlovic, D., Sinninghe Damsté, J.S., de Leeuw, J.W., 1993. Nickel boride: An improved desulphurizing agent for sulphur-rich geomacromolecules in polar and asphaltene fractions. *Org. Geochem.* 20, 901–910.
- Schröder-Adams, C.J., Leckie, D.A., Bloch, J., Craig, J., McIntyre, D.J., Adams, P.J., 1996. Paleoenvironmental changes in the Cretaceous (Albian to Turonian) Colorado Group of western Canada: microfossil, sedimentological and geochemical evidence. *Cretaceous Res.* 17, 311–365.
- Sinninghe Damsté, J.S., Köster, J., 1998. A euxinic North Atlantic Ocean during the Cenomanian/Turonian anoxic event. *Earth Planet. Sci. Lett.* 158, 165–173.
- Sinninghe Damsté, J.S., Rijpstra, W.I.C., de Leeuw, J.W., Schenck, P.A., 1989. The occurrence and identification of series of organic sulphur compounds in oils and sediment extracts: II. Their presence in samples from hypersaline and non-hypersaline palaeoenvironments and possible application as source, palaeoenvironmental and maturity indicators. *Geochim. Cosmochim. Acta* 53, 1343–1355.
- Sinninghe Damsté, J.S., Wakeham, S.G., Kohnen, M.E.L., Hayes, J.M., de Leeuw, J.W., 1993. A 6000-year sedimentary record of chemocline excursions in the Black Sea. *Nature* 362, 827–829.
- Sirevåg, R., Buchanan, B.B., Berry, J.A., Throughton, J.H., 1977. Mechanisms of CO₂ fixation in bacterial photosynthesis studied by the carbon isotope technique. *Archives Microbiol.* 112, 35–38.
- Slingerland, R., Kump, L.R., Arthur, M.A., Fawcett, P.J., Sageman, B.B., Barron, E.J., 1996. Estuarine circulation in the Turonian Western Interior Seaway of North America. *Geol. Soc. Am. Bull.* 108, 941–952.
- Sohl, N.F., 1967. Upper Cretaceous gastropod assemblages of the Western Interior of the United States. In: Kauffman, E.G., Kent, H.C. (Eds.), *Paleoenvironments of the Cretaceous Seaway in the Western Interior*. Colorado School of Mines, Special Publication, pp. 1–37.
- Summons, R.E., Powell, T.G., 1986. *Chlorobiaceae* in Paleozoic seas revealed by biological markers, isotopes and geology. *Nature* 319, 763–765.
- Summons, R.E., Powell, T.G., 1987. Identification of aryl isoprenoids in source rocks and crude oils: biological markers for the green sulfur bacteria. *Geochim. Cosmochim. Acta* 51, 557–566.
- Tissot, B.P., Welte, D.H., 1984. *Petroleum Formation and Occurrence*. Springer, Berlin.
- Veevers, J.J., 1984. *Phanerozoic Earth history of Australia*. Clarendon Press, Oxford.
- Wignall, P.B., Myers, K.J., 1988. Interpreting benthic oxygen levels in mudrocks: a new approach. *Geology* 16, 452–455.
- Wolfe, D.G., 1989. *The stratigraphy and paleoenvironments of middle Cretaceous strata along the central Arizona–New Mexico border*. MSc Thesis, University of Colorado, USA.